

THERMAL ANALYSIS ON PERMAFROST SUBSIDENCE ON THE NORTH SLOPE OF  
ALASKA

By

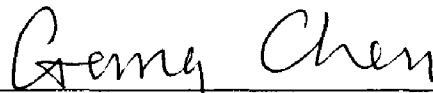
Neha Dinesh Agrawal

RECOMMENDED:



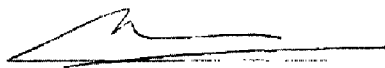
---

Dr. Shirish Patil  
Advisory Committee Chair



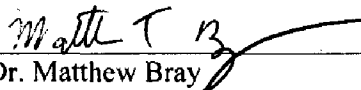
---

Dr. Gang Chen  
Advisory Committee Co-Chair



---

Dr. Abhijit Dandekar  
Advisory Committee Member  
Chair, Department of Petroleum Engineering



---

Dr. Matthew Bray  
Advisory Committee Member

12-18-2015

---

Date

THERMAL ANALYSIS ON PERMAFROST SUBSIDENCE ON THE NORTH SLOPE OF  
ALASKA

A

PROJECT

Presented to the Faculty  
of the University of Alaska Fairbanks

in Partial Fulfillment of the Requirements  
for the Degree of

MASTER OF SCIENCE

By

Neha Dinesh Agrawal, B.E.

Fairbanks, AK

November 2015

*Dedicated to my sister*

# CONTENTS

1	INTRODUCTION .....	1
1.1	Background .....	1
1.2	Problem .....	3
2	LITERATURE REVIEW .....	4
2.1	Background .....	4
2.2	Loading Mechanisms in Thawed Permafrost.....	5
2.2.1	Phase change Contraction (Excess ice Melting).....	6
2.2.2	Consolidation with Fluid Flow.....	6
2.2.3	Stiffness Reduction.....	7
2.2.4	Pore Pressure Reduction.....	7
2.3	Prevention.....	8
2.3.1	Special Packer Fluids.....	8
2.3.2	Insulated Tubing/Casing.....	9
2.3.3	Refrigeration and Heat Pipes.....	9
2.4	Analytical Approach .....	10
2.5	Modeling Heat Transfer in Permafrost.....	10
2.6	Permafrost Lithology Model Parameters .....	11
2.7	Thermal Modeling.....	13
3	FLAC MODELING PROCEDURE.....	15
3.1	Introduction .....	15
3.2	Input Data and Properties.....	17
3.2.1	Mechanical Properties .....	17
A.	Stress Conditions.....	17
B.	Friction Angle: .....	18
C.	Poisson's Ratio.....	19
D.	Young's Modulus.....	19
E.	Cohesion:.....	20
3.2.2	Thermal Properties .....	21
A.	Thermal Conductivity .....	22
B.	Specific heat.....	24
C.	Coefficient of Linear Thermal Expansion.....	26

D.	Cement Properties .....	26
E.	Casing Properties.....	29
3.3	Thermal Model Methodology .....	29
	Stepwise Procedure for Modeling (Small Model).....	29
4	RESULTS AND ANALYSIS .....	33
4.1	Big Model Analysis (Model 1).....	33
4.2	Boundary Conditions for Small Model:.....	34
4.3	Small Model Analysis: Model 2.....	36
4.4	Small Model Analysis: Model 3.....	39
4.5	Steam Injection.....	43
4.6	Big Model Results .....	43
4.7	Small Model Analysis .....	43
4.8	Sensitivity Analysis.....	46
4.9	Comparisons.....	49
4.10	Mitigation Techniques: .....	51
5	CONCLUSIONS AND RECOMMENDATIONS .....	52
5.1	Conclusion.....	52
5.2	Recommendations .....	53
6	REFERENCES .....	54

LIST OF FIGURES

Figure 1. Distribution of Permafrost (<http://pubs.usgs.gov/pp/p1386a/notes-fig6-1.html>) ..... 2

Figure 2. Schematic of thaw consolidation process (Malcolm A. Goodman , 1978) ..... 6

Figure 3. 3D Model (Schematic)..... 15

Figure 4. Schematic of the FLAC model ..... 16

Figure 5. Axi-symmetric Model in FLAC Schematic..... 17

Figure 6. Cohesion vs. Temperature used for cohesion values in FLAC Models (N. A. Tsytovich 1975) 21

Figure 7. Thermal conductivity concept basic schematic ..... 22

Figure 8. Specific Heat Spike incorporated in FLAc model to incorporate the latent heat for melting ice at 273K..... 26

Figure 9. Grid Mesh for small model in FLAC ..... 30

Figure 10. Unbalanced Force (FLAC) to balance forces resulting from simulation..... 31

Figure 11. Big Model Grid Mesh..... 34

Figure 16. Silt-Sand Temperature Distribution over a distance of 20 m from the center of the wellbore. 39

Figure 17a. 1 year Silt - Sand Profile..... 40

Figure 21. Silt – Sand : Temperature Distribution over a distance of 20 m from thr center of the wellbore  
Temperature Distribution Sand..... 44

Figure 22. Clay - Silt: Temperature Distribution over a distance of 20 m from thr center of the wellbore  
Temperature Distribution Sand..... 45

Figure 23. Silt Thaw Radius at 343 K and 383 K for comparison..... 45

Figure 24. Sand Thaw Radius at 343 K and 383 K for comparison ..... 46

Figure 26. Plot of thaw radius for Sand sensitivity analysis of lower and higher values thermal  
conductivity values than the base case..... 48

Figure 27. Plot of thaw radius for Silt sensitivity analysis of lower and higher values thermal conductivity  
values than the base case..... 49

Figure 28. Comparison among different Models ..... 50

## LIST OF TABLES

Table 1. Soil Index Properties (Matthews and Zhang, 2012) .....	16
Table 2. Pressure Gradients used in the FLAC model for boundary conditions.....	18
Table 3. Input Data For FLAC Model .....	19
Table 4. Thermal Conductivity Values for Input Properties in FLAC model.....	24
Table 5. Specific Heat Values - Input Properties.....	25
Table 6. Properties of Gypsum-based cement (Paolo Gardoni, 2011).....	28
Table 7. Properties of Steel Casing used in FLAC (Singh, Probjot et al. 2007).....	29
Table 8. Thaw Radius and boundary conditions at a distance of 20m for small model from.....	35
Table 9. Thaw Radius – Silt from the small model after applying boundary conditions.....	37
Table 11. Thaw Radius and boundary conditions for small model from Big Model (Steam Injection).....	43
Table 12. Lower and Higher Conductivity Values for Sensitivity Analysis .....	47
Table 13. Sand: Thaw Radius from Sensitivity Analysis in response to changes in thermal conductivity	47
Table 14. Sand: Thaw Radius from Sensitivity Analysis in response to changes in thermal conductivity	48

## ACKNOWLEDGEMENTS

This project would not have been possible without the kind support and help of many individuals and organizations. I would like to extend my sincere thanks to all of my committee members. I am highly indebted to the University of Alaska Fairbanks, Department of Petroleum Engineering for giving me the opportunity to do this project. I would like to thank my advisor, Dr. Shirish Patil, for giving me this project and for his constant guidance. I would like to express my sincere gratitude to Dr. Gang Chen for his constant supervision and support in completing the project. Further, I would also like to thank Dr. Dandekar and Dr. Matthew Bray for their guidance and support. I would like to express my special thanks to industry representative Dr. Yanhui Han for giving me such attention and time.

I would like to express my gratitude towards my parents and my sister for their kind cooperation and encouragement which helped me in completing this project. My thanks and appreciation also go to my colleague Kai Wang for developing the project with me and all the people who have willingly helped me out with their abilities.



## ABSTRACT

One of the major problems associated with the oil fields on the North Slope of Alaska is thawing permafrost around producing oil wells. In these wells, the heat from the producing well fluid gradually thaws the permafrost. This thawing in turn destroys the bond between the permafrost and the casing and causes instability that results in permafrost subsidence which further causes subsidence of the soil surrounding the wellbore and, subjects the casing to high mechanical stresses.

The above problem has been addressed by several engineers, and several preventive measures, such as controlling the subsidence by refrigeration or by insulation of the wellbore, have been analyzed. Understanding the thermal behavior of the permafrost is imperative to analyzing permafrost subsidence and providing preventative measures.

The current project focuses on building a scaled-down axi-symmetric model in FLAC 7.0 that will help us understand the thermal behavior (i.e., the heat input to the permafrost interval due to hydrocarbon production) and temperature distributions that result in permafrost subsidence. The numerical analysis estimated the thaw influence of steam injection used for heavy oil recovery and its effect on the area around the wellbore for 10 years. The developed model was compared with Smith and Clegg (1971) axi-symmetric model and COMSOL model and correlations of thaw radius and wellbore temperatures were obtained for different types of soils. Heat transfer mitigation techniques were also attempted which are discussed in the report further.

# 1 INTRODUCTION

## 1.1 Background

Permafrost is defined on the basis of temperature as rock or soil with or without organic matter that has remained frozen continuously for 2 years or more. About 25% of the world land surface is underlain by permafrost, which includes more than 60% of the land surface in Russia, more than 80% in Alaska, and more than 60% in Canada (Kresten, 1969). Permafrost is further classified into two major zones called the continuous zone and the discontinuous zone. The continuous zone is underlain by permafrost everywhere, while the discontinuous zone has many permafrost-free regions. Figure 1 shows the extent of continuous and discontinuous permafrost with sporadic unfrozen zones. Most people are unaware of the existence of this permafrost and the damage it is capable of causing. It can cause special engineering problems for the design, construction, and maintenance of all types of structures. It is critical to take the presence of permafrost into consideration before building or constructing in a permafrost region because lack of knowledge of this can result in tremendous maintenance and relocation costs or even abandonment of highways, railroads, and other structures. To avoid such problems, appropriate measures need to be followed as discussed further in the report.

The thickness of the permafrost depends on the mean surface temperature and the thermal gradient. The lower the temperature and geothermal gradient, the greater the thickness of the permafrost. The thickness also depends on factors like surface vegetation, lakes, and roads, among others. However, it takes decades for these factors to affect the bottom of the permafrost. The active layer is the layer that undergoes seasonal thawing and freezing every year. Seasonal frost penetrates down to the permafrost in most places. However, if it does not, then an unfrozen zone called a talik is formed (Goodman, 1977).

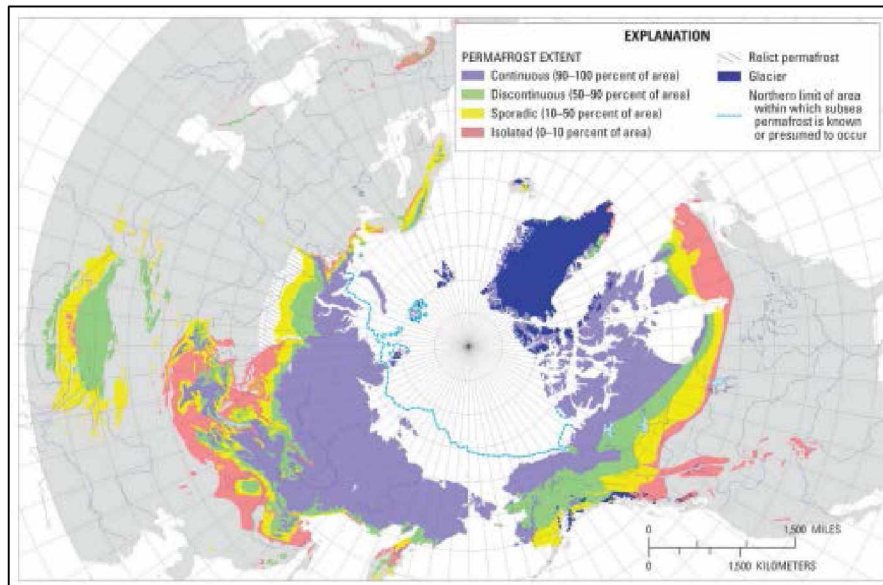


Figure 1. Distribution of Permafrost (<http://pubs.usgs.gov/pp/p1386a/notes-fig6-1.html>)

Exploring in such regions for oil and gas reserves has been challenging from drilling, completion, and operation perspectives. A key issue in completing wells in these regions is how to manage the impact of thaw subsidence of permafrost layers throughout the expected life of these wells.

Engineers face numerous of problems such as permafrost subsidence during drilling, completion, and production operations in the permafrost. Unless some means are used to prevent the heat from affecting the permafrost, these operations possibly result in thaw subsidence.

Drilling through deep permafrost involves a complex thermal/mechanical interaction among the fluids, drill string, and the formation. Improper drilling through the permafrost can result in extensive washouts, fill on bottom, and stuck pipe. At first, refrigerated fluids were tried to solve this problem. However, they proved to be expensive and impractical. Currently, the method used is drilling through the permafrost as fast as possible in order to minimize thaw and wellbore

instability, after which casing can be set and the deeper drilling can be carried out using the normal drilling procedures.

## 1.2 Problem

The problem arises when flowing warm oil is produced from deep formations, transferring heat as it passes through the permafrost and resulting in possible soil settlement. The magnitude of this soil settlement depends on the nature and physical characteristics of the soil and the stress conditions existing in the permafrost. The flow of heat from the warm production wells to the surrounding formations will clearly be a function of the temperature difference between the produced fluids and the formation, the nature of the wellbore completion, and the thermal properties of the formation. It is a challenge to figure out the readjustments caused in the soil due to increased thawing of permafrost over a span of time. The main problem is to predict the magnitude and distribution of this readjustment and the resultant loading on the well casing.

Soil movement due to thawing can be attributed to one or more of the following main reasons (Mitchell and Goodman, 1978):

- 1) The soil contains segregated excess ice.
- 2) The soil, when frozen, is unconsolidated relative to the present overburden.
- 3) The soil contains zones of low permeability or there is an inadequate water supply such that the void caused by the phase change of ice to water cannot be filled, causing a reduction in pore pressure.

## 2 LITERATURE REVIEW

### 2.1 Background

Producing warm hydrocarbons through wells that penetrate permafrost intervals will cause gradual warming of the surrounding formations or, in other words, thawing of the permafrost. It is important to note that as a radial thaw advances from each well, the ice occupying the pore spaces in the frozen/partially frozen sediments will begin to melt, with the phase change leading to a 9% reduction in volume. This weakening or ice to water phase change contraction of different soil layers will lead to soil deformations, which may include both vertical and horizontal displacements/settlements. These settlements can, in turn, induce high strains on the casing, which might result in the ultimate collapse of the casing. (Matthews et al. 2012; Xie and Matthews, 2011; Degeer and Cathro, 1991; Sengul and Brigham, 1983; Mitchell et al., 1983; Goodman 1977, 1978)

Unless steps are taken to prevent thaw (e.g., use of insulated tubing or the use of active refrigerating systems), all production and injection wells will undergo thawing and casing loads will also be developed (Lin C. J, Wheeler J. D. 1978 & Matthews et al., 2012). Previous assessments have shown that the radial thaw bulb generated within the permafrost layer around individual wells or groups of wells may range in size from a few meters to over 20 meters over a period of 20-25 years (Matthews et al., 2012). The extent of thaw and the magnitude to which the permafrost soil deforms will be much larger in the case of multiple well installations (e.g., well rows with tight well spacing) compared to a single well.

Various authors have worked in the area of wellbore heat transfer analysis. A study has also been done using heat tracing techniques on a well to assess the effects of thaw on subsidence and wellbore deformation (Skoczylas, 2012). However, this approach had the limitation of being able

to model the heat transfer at a single depth. Hence, in order to model the entire cross section of the wellbore, multiple sections at various depths of the wellbore would have to be modeled repeatedly, which would give a discontinuous model. Another possible complication that comes from this model is the thermal gradients. Since these gradients would change rapidly over the course of production methods such as cyclic steam injection, this model would become inaccurate. Using this model at the boundaries of established soil zones in the North Slope of Alaska could give accurate results.

## 2.2 Loading Mechanisms in Thawed Permafrost

The thaw subsidence problem is caused mainly by casing strain and not casing stress. As the permafrost thaws and permafrost deformation occurs, strain is induced on the casing. The casing stress is only a consequence of the casing strain. The induced casing strain is bounded and controlled by the amount of permafrost deformation. In other words, the casing cannot strain any more than the permafrost allows. Goodman , (1978) refers to four permafrost subsidence loading mechanisms for inducing casing strain as shown in the Figure 2 below. Phase change contraction in ice rich soil and consolidation with fluid flow are more likely to occur in surface and near surface soils. Stiffness reduction and pore pressure reduction are important in deep permafrost and generate body force type loads.

In addition, he also examined the effects of lithology and thaw variations on casing loads in the context of these four mechanisms:

- 1) Excess ice melting
- 2) Consolidation with fluid expulsion
- 3) Pore pressure reduction

#### 4) Stiffness reduction.

##### 2.2.1 Phase change Contraction (Excess ice Melting)

The casing strain induced by phase change contraction is due to melting permafrost with excess ice. A void is created in the ground due to the volumetric reduction of the ice, which is equivalent to 9% phase change contraction. Furthermore, compression is generated on the casing due to slumping of the overlying soil as well as uplifting of the underlying soil.

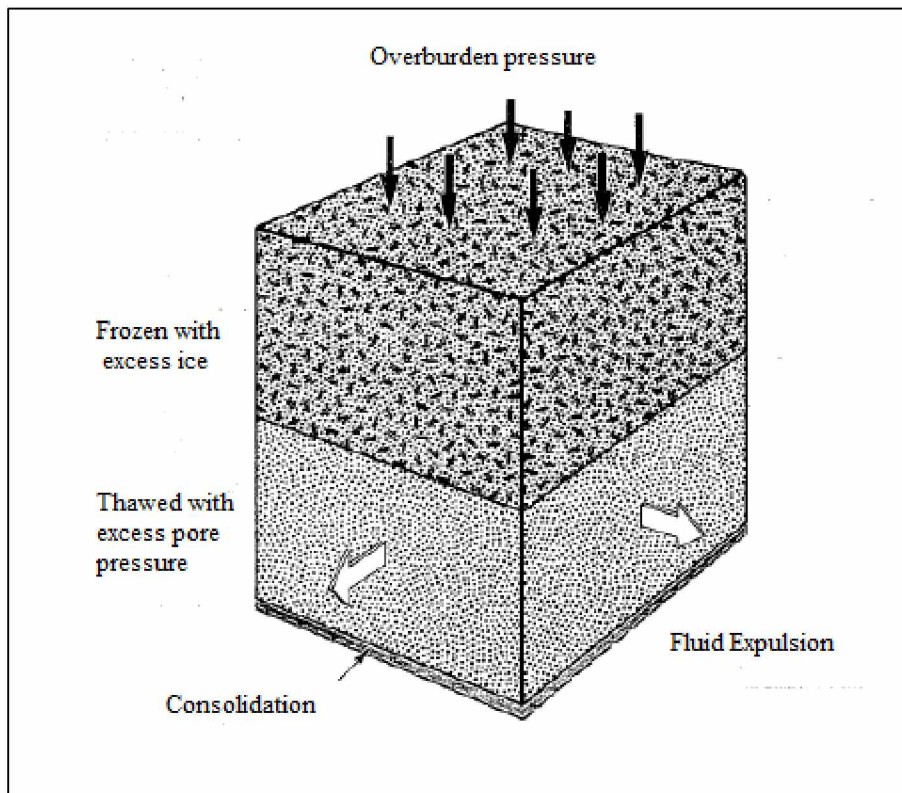


Figure 2. Schematic of thaw consolidation process (Malcolm A. Goodman , 1978)

##### 2.2.2 Consolidation with Fluid Flow

Consolidation with fluid flow is the mechanism where excess pressure is generated upon thaw, causing pore fluid to flow from the excess pore pressure zone and resulting in consolidation of the soil mass. This mechanism implies that the soil is under-consolidated in the frozen state or,

equivalently, contains some amount of excess ice. Also, this excess ice must be greater than 9% of the pore volume; otherwise, there would be a reduction and not an excess of pore pressure, upon thaw. This mechanism is considered a follow-up to the phase change contraction mechanism. Fundamentally, the total deformation consists of two parts: phase change contraction of the excess ice followed by the consolidation with fluid expulsion. The thaw consolidated mechanism is more likely to be near the surface due to the requirement of the excess ice and also a flow path. This theory of thaw consolidation by Goodman and Mitchell, (1978) is basically an extension of the soil mechanics theory of consolidation with appropriate boundary conditions at the thaw front: namely, that any flow from the thaw line is accommodated by a change in volume of the thawed soil. This flow is characterized by Darcy's Law.

### 2.2.3 Stiffness Reduction

The mechanical properties of frozen soil change after thawing since there is stiffness reduction of the soil. This change in stiffness, coupled with the gravity field, is a mechanism for deformation in the thaw subsidence problem. Physically, the stiffness reduction of thawed soil can be caused by the reduction of shear support of the pore ice as it melts in normally consolidated permafrost and/or by melting of small amounts (<9 percent) of excess ice in unconsolidated permafrost. If the thawed and frozen permafrost are considered elastic solids, the stiffness reduction is characterized by a change in the two elastic constants: Young's Modulus ( $E$ ) and Poisson's ratio ( $\nu$ ).

### 2.2.4 Pore Pressure Reduction

The pore pressure reduction is due to shrinkage in volume of pore ice upon thaw. Pore pressure reduction is considered the major mechanism for thaw subsidence in deep permafrost. In



normally compacted permafrost, phase change contraction with thawing of pore ice is accompanied by a decrease in pore pressure, which in turn results in an increase in inter-granular stress and soil compaction. A conservative estimate of pore pressure can be determined by (equation 1) assuming that initial pressure before thaw is hydrostatic head with density  $\rho_i$  and the final pressure of the system. (Goodman, 1978):

$$\Delta p = \rho_i g z \quad (1)$$

Where  $z$  is the depth and  $g$  is the gravitational constant.

### 2.3 Prevention

It is essential to reduce permafrost thaw around Arctic wellbores. The various thermal systems and their unique features and properties used to mitigate the thawing of permafrost around the wellbore are listed below (Goodman and Mitchell, 1978):

- 1) Non-freezing, low water content packer fluids that can be pumped at permafrost temperatures, but gel at producing temperatures to prevent thermal convection and decrease heat loss.
- 2) Double walled insulated tubing/casing that significantly reduces permafrost thaw and can be run with normal handling procedures.
- 3) Refrigerated conductor casing and heat pipes for keeping permafrost frozen and providing surface stability.

#### 2.3.1 Special Packer Fluids

Depending on the permafrost's mechanical behavior, it may not be necessary to prevent thaw, but only to limit it so that induced loads can be tolerated. Although nonfreezing un-gelled fluids such as alcohol, diesel oil, potassium chloride, and calcium chloride solution have been used as

packer fluids in casing-casing annuli opposite permafrost intervals, their insulating properties are not as good as those of gelled fluids (Malcolm A. Goddman, 1978).

### 2.3.2 Insulated Tubing/Casing

Although thaw is reduced with a gelled oil completion, it may not be sufficient for well protection in certain cases, such as ice-rich permafrost, hydrate intervals, close well spacing, or where a previously installed surface casing does not have the required mechanical properties. In addition, cooling the flowing stream may cause hydrate plugging in gas wells and higher viscosity and pressure loss in oil wells. The principal requirement for use of solid insulation is a dry, low-pressure environment. Contact with fluids will irreparably degrade the thermal effectiveness of low density, solid foam systems. Double walled insulated casing has been developed as a means to seal solid insulating materials within the wellbore. This minimizes heat leaks across the thermal short circuit at the coupling. It also allows differential expansion between inner and outer casings. Furthermore, it transfers the weight of each joint of the inner casing to the outer casing that is threaded. Thrust cones and insulated conductor casings are also used, which have their own advantages.

### 2.3.3 Refrigeration and Heat Pipes

Insulation can reduce heat loss and hence permafrost thaw, but cannot prevent it. Refrigeration is required for absolute thaw prevention. Wellbore refrigeration design requires that a minimum refrigeration rate be met at all points along the wellbore. Refrigeration estimates for Arctic wells indicate that some thermal insulation around the production string would have to be provided to keep refrigeration loads down (Davies, 1979). However, a major disadvantage of mechanical refrigeration compared to passive thermal protection methods such as insulation or heat pipes is the requirement for circulation and refrigeration equipment to be on location and maintained.

## 2.4 Analytical Approach

As an alternative to simulation of the heat transfer models built in various modeling software, some authors have also worked to build an analytical approach to analyze heat transfer around the wellbore in a permafrost formation. This analytical approach used commonly available PVT data along with engineering correlations to determine energy balance within the wellbore. However, this approach assumes that the behavior of the fluids in the flow string is a series of steady state conditions. This analytical method considered heat transfer in the flow string to be mainly due to convection and heat transfer in the soil to be based on conduction and permafrost thawing (Howell et al., 1972).

## 2.5 Modeling Heat Transfer in Permafrost

Operators need to recognize that careful planning is required to extend the life of a well during the planning of new well developments in permafrost. Production and injection of wells drilled through permafrost will result in thawing of the permafrost, which will in turn result in permafrost subsidence. Therefore, using a thermal model to simulate thaw over a period of time will help maintain wellbore stability and integrity (Matthews et al., 2012).

According to Matthews and Zhang (2012), a large number of input parameters must be considered in order to build an accurate thermal model, including thermal, soil, and lithological properties. The freezing characteristics and the thaw and deformation response of coarse-grained (gravels and sands) and fine-grained (silts and clays) soil layers tend to differ substantially. For example, the typical high permeability of coarse-grained soils results in an open drainage condition for typical in situ freezing rates. As a result, both void ratios and effective stresses in these soils tend to remain unchanged during freezing; therefore, no excess ice forms in the soil. Similarly, thawing of such soils under an open or free drainage condition will allow access to

free water will result in no changes to the void ratio and effective stresses. However, when a coarse-grained soil exists between two fine-grained layers of low permeability, the thaw column is surrounded laterally by the remaining low permeability frozen soils and a closed/impeded drainage condition will likely exist. Thaw of such soil layers will tend to result in a pore pressure increase, which will inherently increase the soil's effective stresses. Hence, depending on all these factors, the soils will deform/compact somewhat in response to the phase change contraction of the pore ice and corresponding increase in effective stress (Matthew and Zhang, 2012). Thus, fine-grained soils subjected to freeze-thaw cycles behave differently from coarse-grained soils due to inherent differences in ice nucleation/growth and retained permeability.

## 2.6 Permafrost Lithology Model Parameters

While planning the developments of fields in the permafrost areas, operators should include specialized engineering investigations to assess the wells and the risks associated with thaw subsidence. These assessments should clearly define the permafrost soil conditions and examine the relative utility of alternative well completion designs and layouts that may be considered suitable for the prescribed location and field development scenario (Xie and Matthews, 2011; Degeer and Cathro, 1992; Ruedrich et al., 1978; Goodman, 1977). The information required for building an accurate model for thawing of permafrost for a particular field development scenario or well integrity risk assessment includes:

- 1) Lithology profile, which includes soil types, layer thickness, and consolidation state to a depth well below the base of the permafrost
- 2) Physical, thermal, and mechanical properties for the thawed and frozen soil conditions for different types of soil
- 3) Initial in-situ ground temperature profile.

The different input parameters required are divided into three main categories, namely, soil index properties, thermal properties, and mechanical properties. All the properties that fall into these three main categories are listed in the Table 1 below:

<i>Soil Index Properties</i>		
<i>Soil Index Parameters</i>	<i>Thermal Parameters</i>	<i>Mechanical Parameters</i>
Lithology Profile With Depth	Thermal Conductivity, Frozen And Unfrozen	Poisson's Ratio
Moisture Content	Specific Heat, Frozen And Unfrozen	Coefficient Of Lateral Effective Earth Pressure At Rest
Bulk Density	Thermal Conductivity, Frozen And Unfrozen	Hydrostatic Pore Pressure And Pore Pressure Upon Thaw
Pore Water Salinity	Total Latent Heat	Vertical Geostatic Effective Stress
Specific Gravity	Thermal Diffusivity Coefficient	Horizontal Geostatic Effective Stress
In Situ Temperature		Pore Pressure Upon Thaw
Specific Surface Area		Frozen And Unfrozen Modulus
In-Situ Unfrozen Water Content		Friction Angle
Dry Density		Cohesion
Initial Void Ratio		Tension
Initial Porosity		

Table 1. Soil Index Properties from Literature Review (Matthews and Zhang, 2012)

Reasonable estimates can be established for many of the aforementioned parameters based on known geotechnical relationships and/or engineering judgment in conjunction with the geological log data normally acquired during drilling operations. Some parameters can currently

only be determined accurately for a specific site through the acquisition and testing of continuously-cored frozen borehole samples (Matthews and Zhang, 2012).

## 2.7 Thermal Modeling

Several studies describe thermal models for predicting permafrost thaws. The models developed by Marques (2009) and Merriam and others (1975) can be applied only for crude oil production, not for mixtures of gas, oil, and water. Lin and Wheeler (1978) presented equations for simulation of transient heat flow within the wellbore and permafrost formation. The formulation of the problem is general enough to handle most aspects of practical interest. The tests they designed were used to simulate permafrost thaw during drilling and production. Temperature measurements along the surface casing, stream, and in the permafrost around the wells matched their thermal model closely.

Davies et. al. (1979) described a field experiment conducted by BP Alaska Inc. to investigate whether development of a considerable thaw zone around the wellbore would result in soil subsidence or excessive casing stress. The experiment consisted of hot oil circulation in wells drilled in permafrost to achieve a thaw radius around the wellbores. The temperatures and stresses were monitored using techniques such as surface load cells, wireline logs such as temperatures, cement bond, gamma-ray, multiple collar locator, and casing inspection logs. They identified two possible solutions to reduce the thaw radius: circulation of refrigerated fluid and installation of wellbore insulation.

Engineers have two different approaches to the problem of thawing permafrost. The first strategy focuses on well protection and the second emphasizes protection of the permafrost via insulation

(active or passive). The first approach allows the permafrost to thaw but the design of wellbore completion is such that the wellbore is protected from excessive stress, mainly at the casing.

Several authors have examined the relative effectiveness of various insulating materials. Azzola et al. (2004) studied the heat transfer characteristics of vacuum insulated tubing (VIT) using a two-dimensional axi-symmetric physical model. They discovered that the VIT did not have single conductivity value, but had a potentially wide range of conductivity values depending on the boundary conditions. On the other hand, Singh (2007) suggested vacuum insulated tubing for heat retention within sub-sea wellbores in order to minimize wax deposition.

Bunton et al. (1999) also considered the use of vacuum jacketed insulated tubing for steam injection and permafrost applications. This new product allowed more heat to be delivered to the target formation for steam injection-enhanced oil recovery and, in colder climates, prevented permafrost thawing.

Marques et al. (2009) also focused on wells penetrating permafrost for heavy oil recovery. Their experimental components determined thermal conductivity versus temperature of nanomaterials fashioned into insulation (silica aerogels, fiberglass, thermoplastic insulation, and carbon fibers). They developed a comparator thermal conductivity apparatus as well as direct measurements using heat flux sensors. Furthermore, a simplistic experimental simulation explored the role of mechanical stress due to thermal cycling.

### 3 FLAC MODELING PROCEDURE

#### 3.1 Introduction

The following project includes simulations for thermal analysis of permafrost subsidence on the North Slope of Alaska. The simulations were carried out in FLAC 7.0 (Fast Lagrangian Analysis of Continua), which is an explicit finite difference program (computer simulation software package) developed by ITASCA Pvt. Ltd for engineering mechanics computation to solve different engineering problems. The simulation study consisted of three axi-symmetric models having a vertical cross section area as shown in the Figure 3.

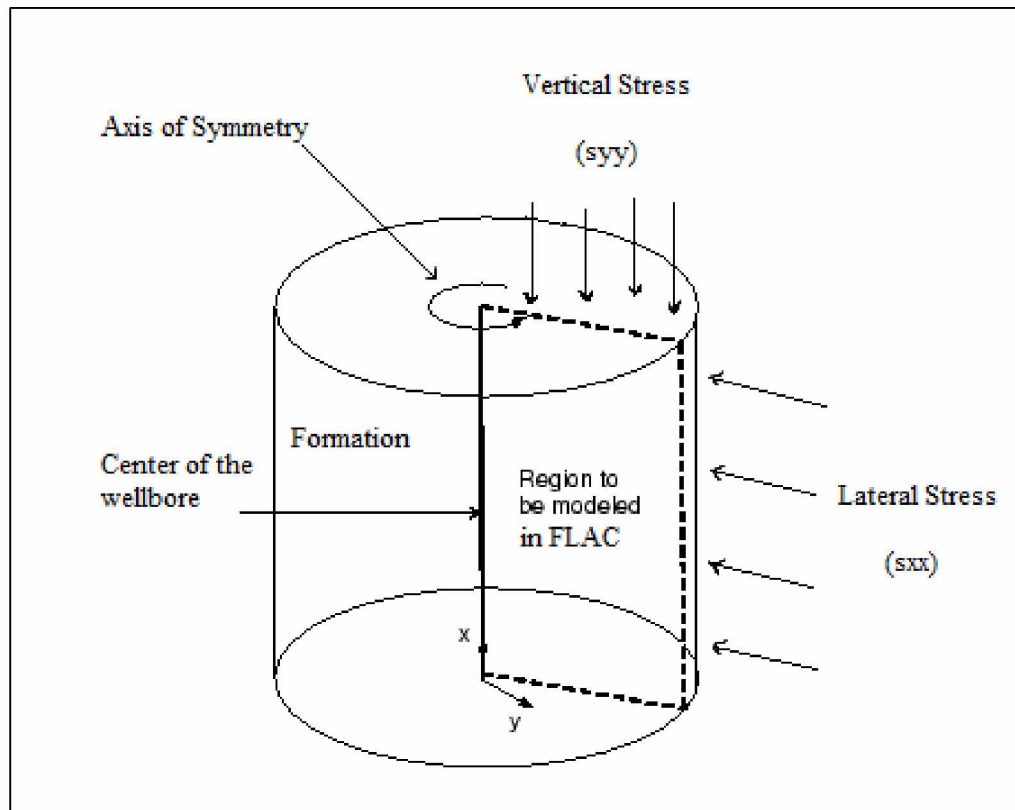


Figure 3. 3D Model (Schematic)



The first model consisted of 600m depth and 100 m width. This model is addressed as the Big Model in the current report. This model was built mainly to cover a wider range of distances from the center of the wellbore and get accurate boundary conditions for the two small models developed further. The second and the third model were based on studying two cross section areas more accurately from the big model (20m X 20m). The second model consisted of a cross section area from 100 m to 120m depth. It included two types of soil: clay and silt. The third model consisted of a cross section area of 280 m to 300 m depth. This model included silt and sand. The small models helped in studying the thawing effects in the near wellbore region more accurately. Using these small models a detailed distribution of formation temperatures in the near wellbore region were obtained. The depths of these models were decided on the basis of a literature review (Mitchell, 1978). Different literature review papers presented different depths, but the range of depths used in the current project was kept more or less the same.

The figure below represents a schematic of the model built in FLAC. The model consists of three layers, namely, clay, silt and sand. Peat was not taken into account because of the inaccessibility of the input parameters needed to define each type of soil.

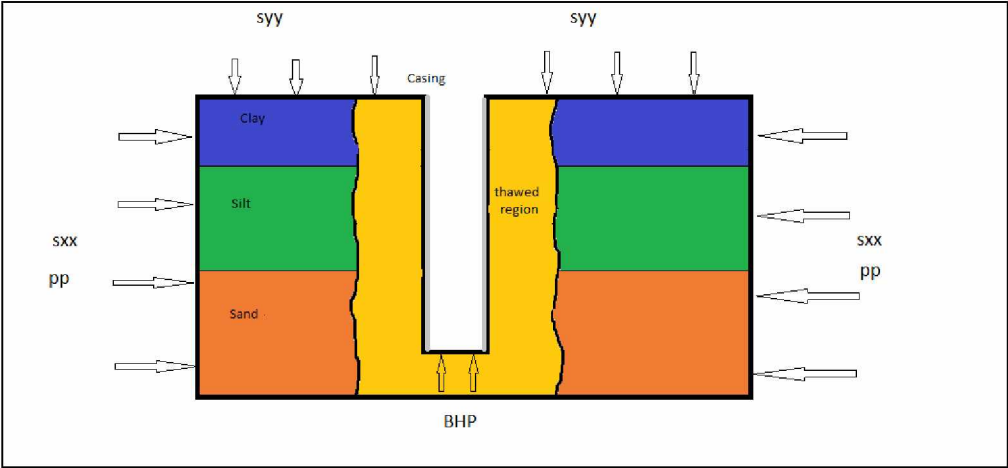


Figure 4. Schematic of the FLAC model

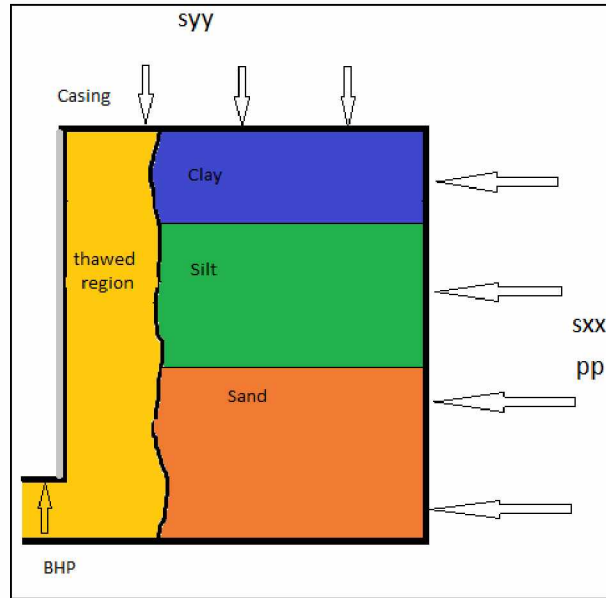


Figure 5. Axi-symmetric Model in FLAC Schematic

### 3.2 Input Data and Properties

The model built in FLAC included mechanical, thermal, and cement and casing properties.

#### 3.2.1 Mechanical Properties

The only way to define a soil type in FLAC is using its mechanical properties. Hence, a coupled cross-section of mechanical and thermal properties was modeled in FLAC. The mechanical properties included soil cohesion, tension, various horizontal and vertical stresses, pore pressures, friction angle, Young's modulus, density, and Poisson's ratio.

##### A. Stress Conditions

According to McLellan (2008), the thaw subsidence problem requires a profile of horizontal in-situ stresses for analysis. Most workers have deemed it acceptable to assume transversely isotropic total horizontal stresses equal to a constant ratio times the vertical stress. Similarly, due to lack of in-situ data, the pore pressure in the ice phase of the permafrost has been assumed to be equal or close to the hydrostatic pressure of a column of water. The Table 2 below

summarizes the stress and pore pressure assumptions made in three papers. It is important to note the assumed  $K_0$  (ratio of horizontal to vertical stress) for permafrost at frozen state was 0.73. The total estimated horizontal stress in the frozen state permafrost was  $14.7\text{KPa}\text{m}^{-1}$ . The original in-situ horizontal stresses reported for permafrost on the Alaskan North Slope used in the current simulation study were as follows (McLellan, 2008):

<i>Reference</i>	<i>Depths</i>	<i>Sv Grad.</i>	<i>Sh Grad.</i>	<i>Frozen Ko</i>	<i>Po Grad.</i>
<i>Perkins et al. (1974) &amp; Ruedrich et al. (1978)</i>	0 – 564 m	20.1KPa/m	14.7 KPa/m	0.73	10.2KPa/m
<i>Goodman and Wood (1975)</i>	0 - 400 m	20.1KPa/m	14.9KPa/m	0.73	9.7KPa/m

Table 1. Pressure Gradients used in the FLAC model for boundary conditions

Where,  $S_v$  and  $S_h$  are the vertical and horizontal stresses respectively and  $P_o$  is the pore pressure.

#### B. Friction Angle:

Soil friction angle is a shear strength parameter of soils. Its definition is derived from the Mohr-Coulomb failure criterion and it is used to describe the shear resistance of soils together with the normal effective stress. In the stress plane shear stress-effective normal stress, the soil friction angle is the angle of the inclination with respect to the horizontal axis of the Mohr-Coulomb shear resistance line. Friction angle, Poisson's ratio, and density values were taken from various frozen ground engineering books (Johnston 1981, N. A. Tsytovich, 2000). The values are given in Table 3.

### C. Poisson's Ratio

Poisson's ratio is defined as the ratio of lateral strain to axial strain. It is given by:

$$v = E_e / E_a \quad (2)$$

Where  $E_e$  is the lateral strain and  $E_a$  is the axial strain. The values of friction angle, density, and Poisson's ratio used for different types of soils are listed in Table 3 (Tsytoovich, 1975).

<i>Soil Type</i>	<i>Friction Angle (degrees)</i>	<i>Density (kg/m<sup>3</sup>)</i>	<i>Poisson's Ratio</i>
Clay	20.0	1800	0.45
Silt	32.1	2000	0.32
Sand	27.8	2100	0.38

Table 2. Input Data For FLAC Model

### D. Young's Modulus

The modulus of elasticity or Young's Modulus of a soil is an elastic soil parameter most commonly used in the estimation of settlement from static loads. Young's Modulus may be estimated from empirical correlations, laboratory tests, undisturbed specimens, and results of field tests. Based on the results of cyclic compression tests on 200-mm cubes of three different soils, Tsytoovich (1975) found that the variation of Young's modulus,  $E$ , with temperature could be represented by the following empirical correlations (Johnston, 1981).

For frozen sand (with total moisture content of 17 to 19%):

$$E = 500(1 + 4.2\Theta) \quad (3)$$

For frozen silt (with total moisture content of 26 to 29%):

$$E=400(1+3.5\theta) \quad (4)$$

For frozen clay (with total moisture content of 38 to 56%):

$$E=500(1+0.46\theta) \quad (5)$$

Where  $E$  is Young's modulus in MPa and  $\theta$  is the number of °C below 0°C.

E. Cohesion:

Cohesion is a component of shear strength of a soil that is independent of the inter-particle friction. The values were calculated from correlations on plots generated using a literature review. The cohesion values were plotted from the Frozen Ground Engineering book (Johnston, 1981). Figure 6 shows temperature dependence of uniaxial short-term compressive strength for various frozen soils (Wolfe and Thieme, 1964).

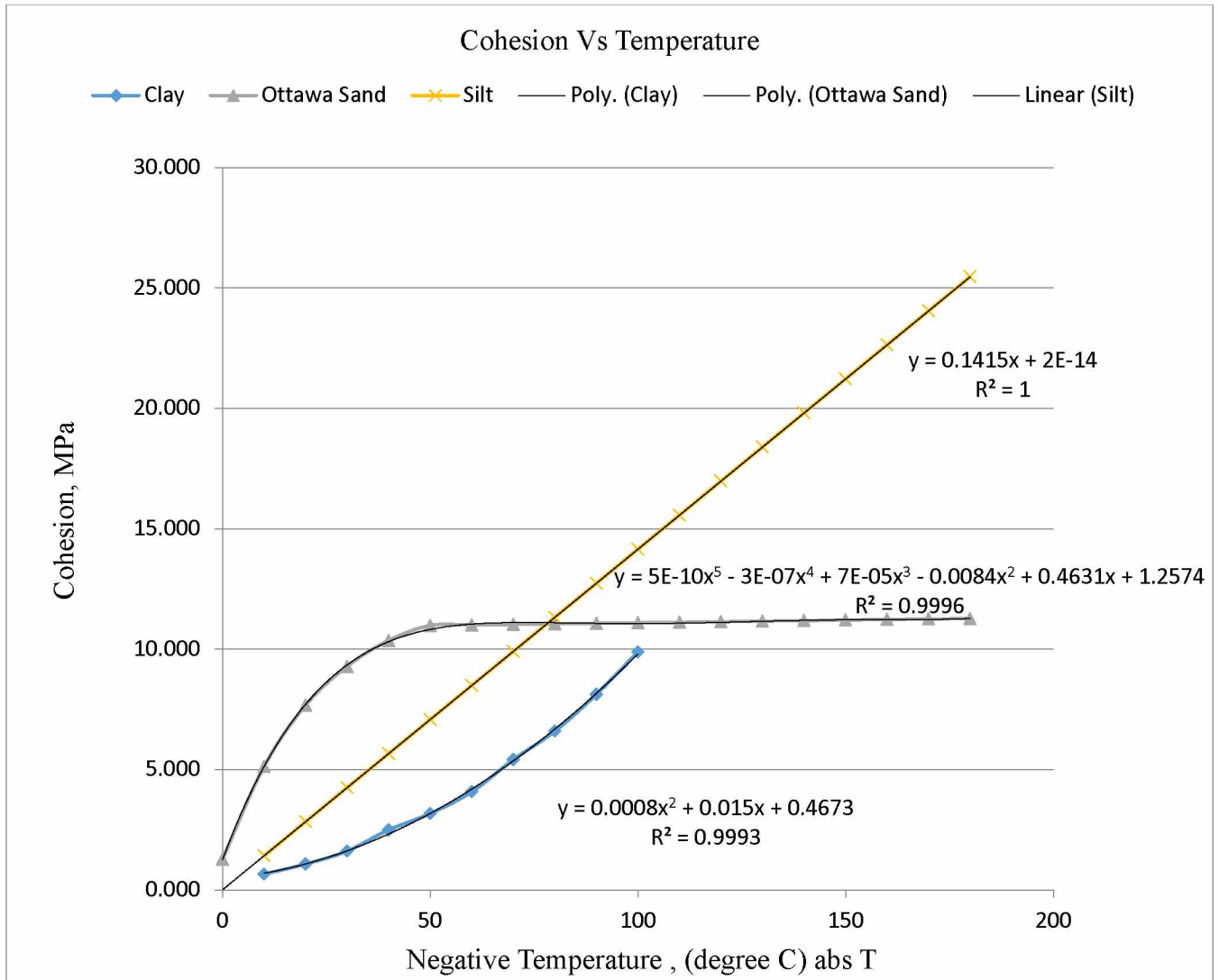


Figure 6. Cohesion vs. Temperature used for cohesion values in FLAC Models (Tsytoovich 1975)

### 3.2.2 Thermal Properties

Soil thermal properties are of great importance in estimating the thaw radius of the permafrost and in other situations where heat transfer takes place in the soil. The thermal properties used in FLAC were thermal conductivity, specific heat, and the thermal expansion coefficient. Latent heat was also incorporated by modifying specific heat over a range of temperatures, which is explained further below. Also, the soil material properties and the boundary conditions often

need to be specified to solve heat transfer problems in actual soil, which was also incorporated into the model. Recently, however, various finite differences techniques have been used to account for fluctuating boundary conditions and variable thermal properties (Xie, 2009).

#### A. Thermal Conductivity

Considering a prismatic element as shown in Figure 7 of soil having a cross sectional area,  $A$ , at right angles to heat flow,  $q$ , and the soil thermal conductivity  $k$  is defined as:

$$k = \frac{q}{A(T_2 - T_1)/l} \quad (6)$$

Where, the temperature drops from  $T_2$  to  $T_1$  over the length of the cross section  $l$ .

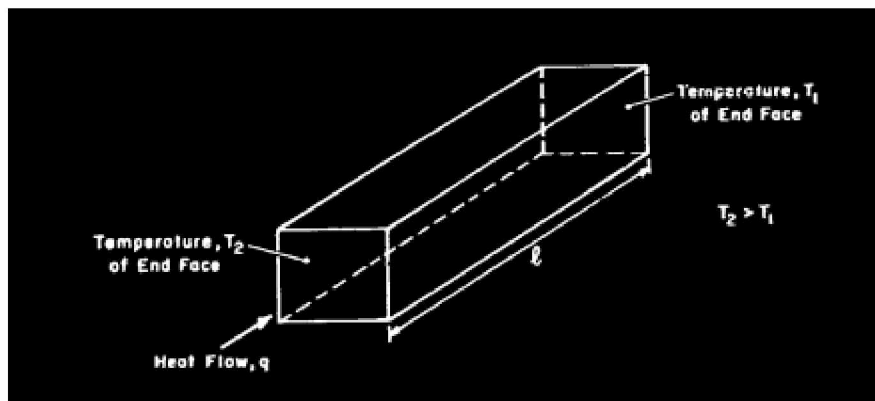


Figure 7. Thermal conductivity concept basic schematic

The definition of thermal conductivity implies a steady state condition in which the temperature at a point does not vary with time. If, however, the temperature is changing with time, it means that the soil itself must be either losing or gaining heat. If the temperature of an element of soil is increasing with time, then some of the heat flow is being used for this purpose, the amount depending on the specific heat of this element.

The thermal conductivity values used in the current simulation were estimated from the following thermal conductivity graphs of unfrozen and frozen coarse- and fine-grained soils by referring to the water content and dry density of the different soils (After Kersten, 1949).

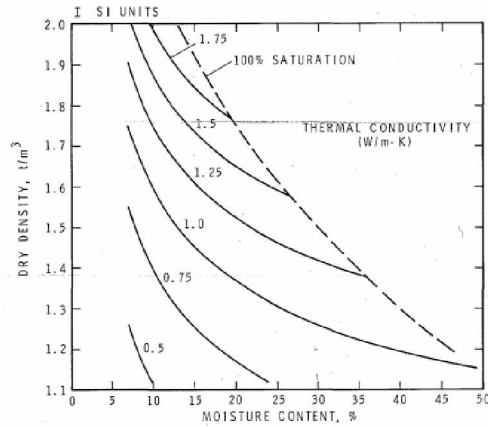


Figure 6a. Thermal conductivity of unfrozen fine-grained soil (After Kersten, 1949)

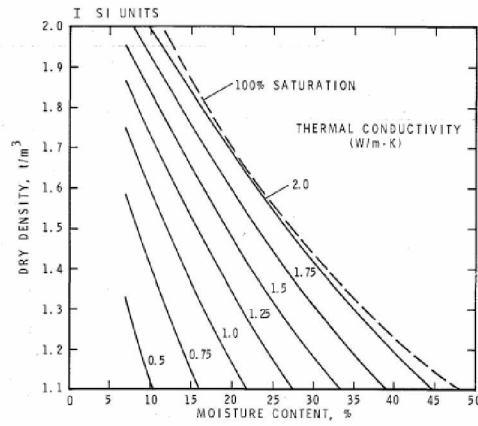


Figure 6b. Thermal conductivity of frozen fine-grained soil (After Kersten, 1949)



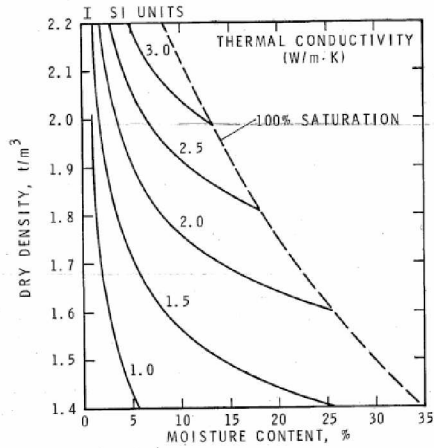


Figure 6c. Thermal conductivity of unfrozen coarse-grained soil (After Kersten, 1949)

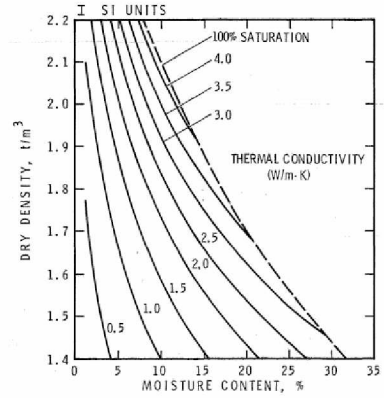


Figure 6d. Thermal conductivity of frozen coarse-grained soil (After Kersten, 1949)

The thermal conductivity values were obtained from figure 6. The fine grain figures (6b. and 6d.) of frozen and unfrozen soils were used for clay and silt at different water contents of 38% for clay and 26 % for silt. Similarly, coarse grained soil (Figures 6a. and 6c.) were used for sand at a water content of 19 %. (Johnston,1981). The thermal conductivity values used are given in Table 4 below:

Soil Type	Thermal Conductivity (W/m K)	
	Frozen	Thawed
Clay	1.242	1.002
Silt	1.956	1.471
Sand	2.208	1.568

Table 3. Thermal Conductivity Values for Input Properties in FLAC model

## B. Specific heat

The specific heat capacity,  $C$ , per unit volume of soil is the heat energy required to raise the temperature of the unit volume by  $1^{\circ}\text{C}$ . The specific heat values used in the current project were

obtained from a literature review (Tsyтович, 2000). The properties used to define the thermal model above are given in Table 5 below:

<i>Type of soil</i>	<i>Specific Heat Values</i> <i>C</i>		<i>Water Content</i> <i>w</i>	<i>Modified Specific Heat Values</i>  (J/kg-K)
	<i>Frozen</i> (J/kg-K)	<i>Thawed</i> (J/kg-K)		
<i>Clay</i>	1100	1460	0.38	72640.8
<i>Silt</i>	1060	1430	0.26	62140
<i>Sand</i>	720	1080	0.19	51072

Table 4. Specific Heat Values - Input Properties

The modified specific heat values are estimated using the equation (Johnston,1981).:

$$C = \rho \times l \times w \quad (7)$$

Latent heat is the energy released or absorbed by the soil (or any thermodynamic system) during a constant-temperature process. It was considered to incorporate the phase transition of the melting ice due to thawing of the permafrost. The latent heat of ice is 333.7 KJ/kg (Johnston, 1981). In equation 7,  $\rho$  is the density of the soil,  $l$  is the latent heat of ice, and  $w$  is the water content.

Since there was no input for any other parameters to account for latent heat, we increased the specific heat values to account for latent heat from 272 to 274 K (Figure 8). The reason for selecting this temperature range was that the permafrost thaws approximately at 273 K (Mitchell, 1978). Hence, a spike of specific heat values was incorporated.

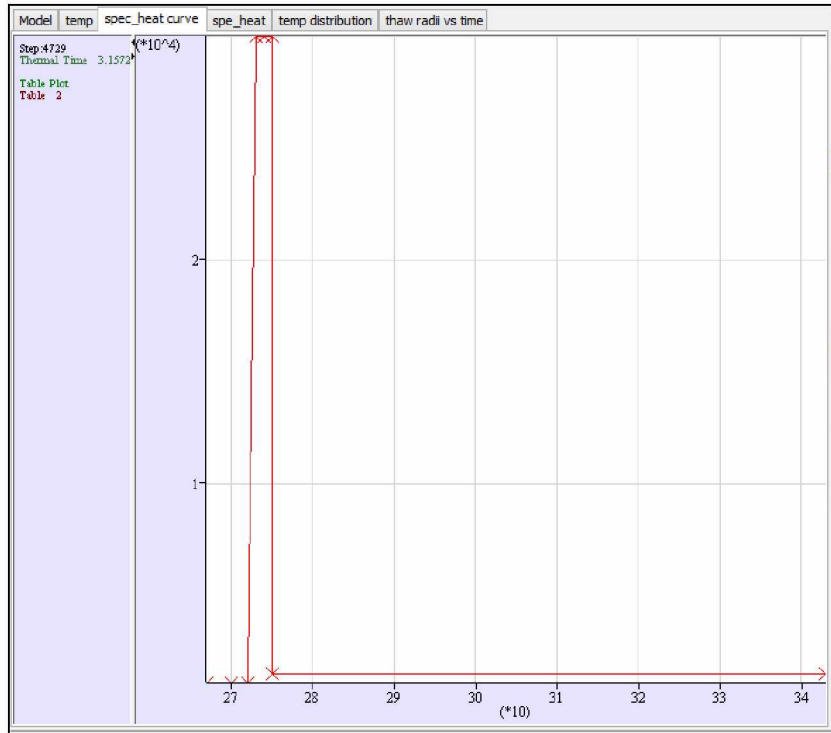


Figure 8. Specific Heat Spike incorporated in FLAc model to incorporate the latent heat for melting ice at 273K

### C. Coefficient of Linear Thermal Expansion

The degree of expansion divided by the change in temperature is called the material's coefficient of thermal expansion, which generally varies with temperature. Due to a lack of data, the thermal expansion coefficient was assumed to be a constant value of  $1.66 \times 10^{-6} \text{ 1/K}$  for all three types of soil (Paolo Gardoni, 2011) since the values of thermal linear expansion coefficient were in the same range and varied by a small magnitude for different soils.

### D. Cement Properties

Cementing of casing in the permafrost on the Alaskan North Slope presents problems to many operators (Goodman et al., 1978). Primarily, the cement system must be kept from freezing until

after the setting reaction is complete. Different types of systems have been suggested and used to solve this problem.

Since the discovery of the Prudhoe Bay field in 1968, research in Arctic cements has been extensive. Today, wells drilled through permafrost can be cemented routinely with specially formulated cements that provide a high amount of strength, good bonding, and wait times of 16 hours or fewer. Positioned between permafrost and casing, Arctic cement must have certain special properties. Operators on the North Slope requested a cement system that could be mixed, pumped, and placed conventionally behind the pipe set through the permafrost. The cement should set to compressive and bond strengths sufficient to support the pipe and prevent the circulation of drilling fluids up the annulus as drilling is continued. It was further requested that the cement system placement technique be kept as simple as possible due to the adverse working conditions present on the North Slope. These cements must hydrate and set at sub-freezing temperatures to support the casing and bond to the formation, and must not degrade because of freeze-thaw cycles of permafrost over the life of a well. Arctic cements must also gain sufficient strength to support compressive and tensile loads generated by thaw-subsidence.

In permafrost environments, conventional oil wells (Portland cement) may not set easily unless the environmental temperatures are maintained above the freezing point (Goodman et al., 1978). This promoted the introduction of gypsum-based cements and high alumina-based cements for Arctic well completions.

Desirable characteristics for permafrost applications are the following:

- 1) Short waiting on cement (WOC) time

- 2) Ability to set at existing borehole temperatures without excessive heating of mixing or displacing water
- 3) Ability to set with low heat of hydration to prevent additional permafrost melting
- 4) Ample placement (thickening) time
- 5) Sufficient strength development for well operations.

Gypsum-based cement was used in the current project. Gypsum based cements are blends of a controlled-set gypsum cement, API Class G cement, salt for freeze-point depression, a dispersant, a chemical dispersant, and a chemical additive to control thickening time. A 60% gypsum and 40% Class G blend is commonly used in the Alaskan and Canadian Arctic. Gypsum provides early strength, even at low temperatures, while the class G constituent gives additional later strength.

The slurries of these cements can be prepared by mixing cold cement with cold water and are designed to set at temperatures between 15° and 80°F (Goodman et al., 1978).

<i>Density</i>	2300	Kg/m <sup>3</sup>
<i>Elastic Modulus</i>	$3.750 \times 10^{10}$	Pa
<i>Poisson's Ratio</i>	0.249	-
<i>Thermal Conductivity</i>	1.73	W/mK
<i>Specific Heat</i>	900	J/kg-K
<i>Thermal Expansion Coefficient</i>	$1.0 \times 10^{-7}$	1/K

Table 5. Properties of Gypsum-based cement (Paolo Gardoni, 2011)

## E. Casing Properties

For FLAC modeling, a steel casing was used, with the properties given in Table 7. These properties were obtained from literature review (Singh, Probjot et al. 2007).

<i>Density</i>	6525.325	Kg/m <sup>3</sup>
<i>Elastic Modulus</i>	2.830×10 <sup>7</sup>	Pa
<i>Poisson's Ratio</i>	0.279	-
<i>Thermal Conductivity</i>	16	W/mK
<i>Specific Heat</i>	486	J/kg-K
<i>Thermal Expansion Coefficient</i>	1.2×10 <sup>-7</sup>	1/K

Table 6. Properties of Steel Casing used in FLAC (Singh, Probjot et al. 2007)

### 3.3 Thermal Model Methodology

The thermal model in FLAC incorporates both conduction and advection models. The conduction models allow simulation of transient heat conduction in a material and the development of thermally induced stresses.

The modeling procedure explained below is mainly for the small model. The difference in the small model and the big model were the grid cell widths. The big model had bigger grid cell widths; hence, cement and casing were not added to it. The main purpose of the big model was to get the boundary temperatures for the small model. Since the small model was more detailed, the procedure has been written with respect to the small model.

#### Stepwise Procedure for Modeling (Small Model)

- 1) The first step of FLAC is to build a grid. In the current model, this grid is 40×40 cells.

These grid cells were chosen to in order to be able to assign properties to cement and

casing and make sure that proper thicknesses were available for excavation (adding wellbore into the formation).

- 2) In order to critically analyze the near wellbore region, the grid cells were arranged by changing their specific ratio (Figure 9) where specific ratio is the ratio between the grid cell width and height.

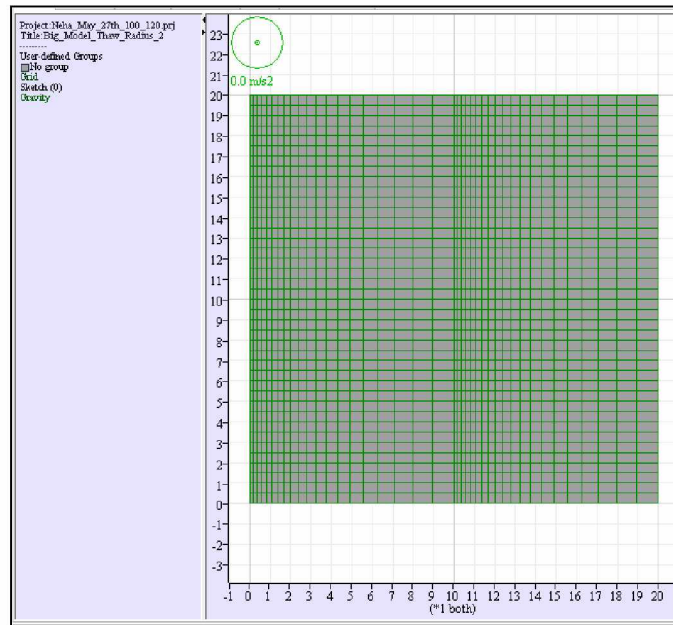


Figure 9. Grid Mesh for small model in FLAC

- 3) The next step was to define the material properties of each soil. Hence, the Mohr Coulomb Model was used to make the model more accurate by having both elastic and plastic input parameters. The elastic properties used in the model were elastic modulus and Poisson's ratio, which the model used to calculate the bulk modulus and the shear modulus. The plastic properties inputted were cohesion, tension, and friction angle of the soils.

- 4) The bottom boundary of the grid was fixed in the y-direction to prevent any movement in that direction. The x-direction boundary was fixed on the left to prevent any movement there since it was also the axis of symmetry in the axi-symmetric model.
- 5) Horizontal and vertical stresses and pore pressure were calculated using the gradients from the literature review and were applied to their respective boundaries.
- 6) The next step was to build the gravitational loading, which was specified by a global setting in the model via the settings modeling tool tab. The value was  $9.81 \text{ m/s}^2$ , which was listed as the magnitude of gravitational acceleration constant.
- 7) Furthermore, it was anticipated that large deformations would occur in the current analysis and hence the strain was adjusted to be large via Mechanical Settings.
- 8) The elastic model was then run to initial equilibrium to balance all the unbalanced forces in the model, as shown in Figure 10.

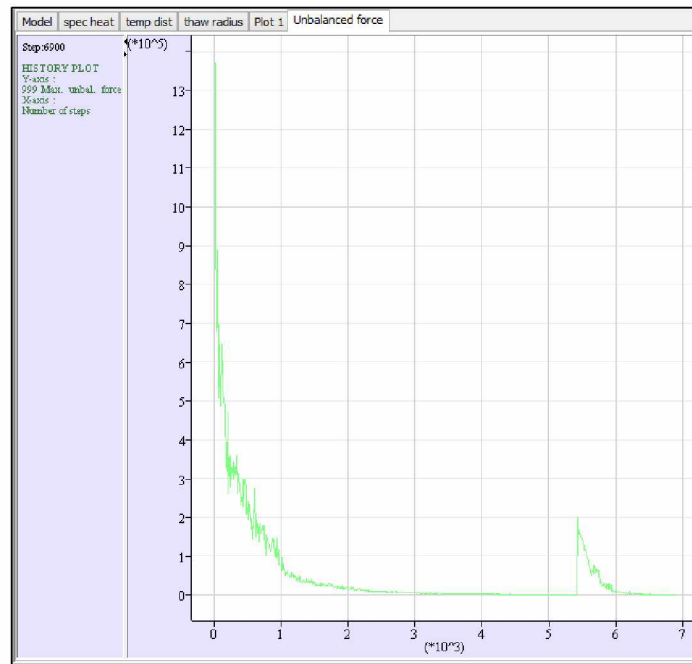


Figure 10. Unbalanced Force (FLAC) to balance forces resulting from simulation



- 9) Then the wellbore was excavated and cement and the casing properties were added into the model via material properties.
- 10) The thermal properties of thermal conductivity, specific heat, and thermal expansion coefficient were then added using thermal material properties. The thermal properties were assumed to be isotropic for each type of soil.
- 11) The temperatures from the big model were then used in the small model to study a more accurate temperature distribution.
- 12) The small model was allowed to simulate for a period of 30 years by controlling the age of the model, and results were obtained over different time periods.
- 13) Then, the graphs were plotted to get a better view of the results and the temperatures were read more accurately using the information tab. Lastly, the results obtained were analyzed.

## 4 RESULTS AND ANALYSIS

### 4.1 Big Model Analysis (Model 1)

The main purpose of the big model was to get boundary conditions for the small model, while the main objective of the small model was to study the temperature distribution around the wellbore and to determine the thaw radius of the permafrost formation over a period of 30 years. Since the thaw radius after 30 years will reach a distance much greater than the small model dimensions the simulation was carried out only up to 30 years. On the other hand, the dimensions of the small model could not be changed due to the specific grid cell widths required for adding cement and casing properties.

The axi-symmetric geometry in FLAC is used to approximate the post-production state of the permafrost formation. The axi-symmetry provides an analysis of thaw radius around the wellbore closely related to the three-dimensional condition.

The big model consisted of three layers of soils. The first layer was clay that extends from the surface to 195m. The second layer consisted of silt from 195m to 285m. Lastly, the third layer consisted of sand from 285m to 600m (Figure 11).

The material properties used for the soil types, casing, and cement were taken from an extensive literature review (Gardoni, 2011; Mitchell, 1978). These material parameters used to define each of the soil types included mass density, bulk modulus, shear modulus, Poisson's ratio, elastic modulus, cohesion, tension, friction angle, and dilation angle. The initial temperature was taken to be 262K based on the literature review and on the correlations used to estimate the input parameters required by FLAC. The simulation included two wellbore temperatures, 343K and 383K. To study the effect of steam on the temperature distribution around the wellbore, 383K

was also included. Casing and cement were also included in the model. Steel casing properties were used to define the casing and Gypsum cement was used.

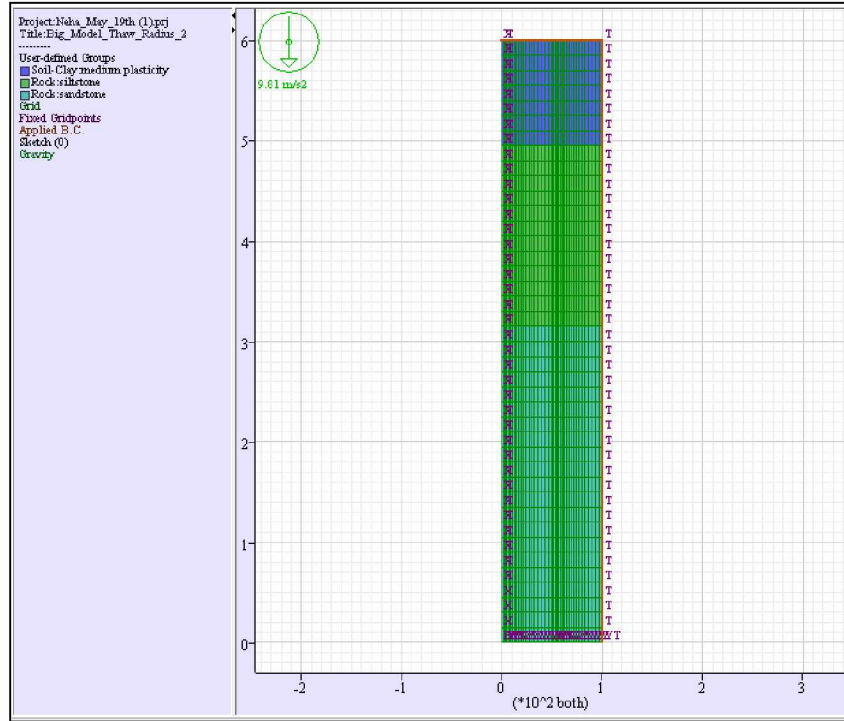


Figure 11. Big Model Grid Mesh

#### 4.2 Boundary Conditions for Small Model:

The thaw radii obtained from the big model for 343K were as given in table 8. The temperatures at 20 m from the center of the wellbore for the small model were also determined, as shown in Table 8. The permafrost thaws at 273 K thereby increasing the temperature and causes changes in stresses and overburden stresses in the near wellbore region (Goodman, 1978). These temperatures at a distance of 20 m from the center of the wellbore were taken from the big model and were used as boundary conditions in the small model to get more accurate temperature distributions in the near wellbore region.

		<i>At 20 m from Big Model</i>
<i>Years</i>	<i>Thaw Radius (m)</i>	<i>Temperature for small Model – Boundary Conditions</i>
1	6	262
2	8	262.8
3	9.1	263.7
4	10	264.7
5	10.5	265
7	11	266
10	11.8	267
12	12.2	268
15	13	268.2
17	13.6	269
20	14.2	269.5
22	14.5	270
25	15.25	270.5
27	16	271
30	16.5	271.2

Table 7. Thaw Radius and boundary conditions at a distance of 20m for small model from Big Model

The Figure 12 shows that the thaw radius increases rapidly in the beginning of the production period and then begins to slow down. This is because the thaw radius stabilizes after some decades (i.e it approaches thermal equilibrium) due to changes in soil properties such as thermal conductivities of frozen soil and unfrozen soil. Hence, the heat does not dissipate to a farther distance from the wellbore.

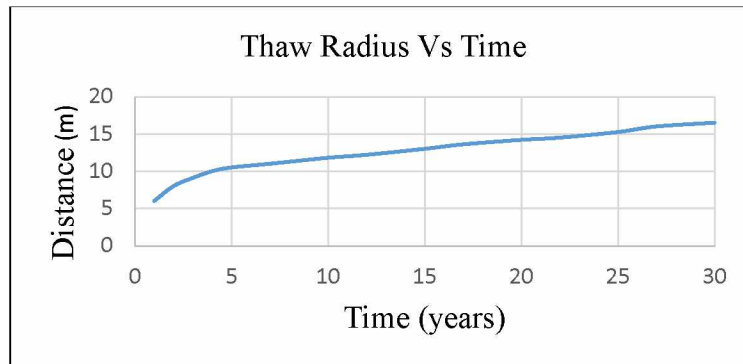


Figure 12 Thaw Radius vs. Time for Big Model

#### 4.3 Small Model Analysis: Model 2

The small models consisted of two cross-sections, as mentioned above. The first cross section was a 20m depth model (20m×20m) consisting of clay and silt. The main objective of this model was to get the thaw radius and temperature distributions of the clay and silt formation. The temperatures simulated in the big model were used to study the distribution of the temperatures and determine the thaw radius in the small model more accurately. Figure 13 shows the model layout for the small model. The boundary conditions for the small model were obtained from the big model, i.e. the temperatures at a distance of 20 m from the center of the wellbore or the axis of symmetry (refer to Table 8).

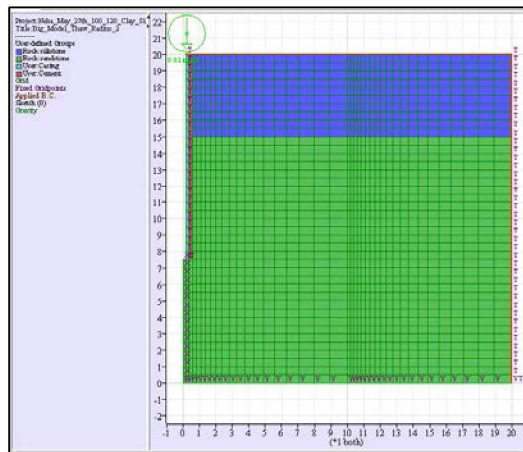


Figure 13. Small Model Mesh

Figure 14, below shows the temperature distribution around the wellbore over a period of 30 years. In order to make the graph clear and visible, only certain years were plotted, which were spread out over a period of 30 years. From the graph, we can see how the temperature increases over the time span of 30 years. In addition, we can also see the shifting of the temperature curve as the number of year's increases gradually due to the changing properties. The red line in the

figure 14 is an isotherm of 273 K to show the thaw radius increase over the time. The thaw radius of clay - silt is given in Table 9.

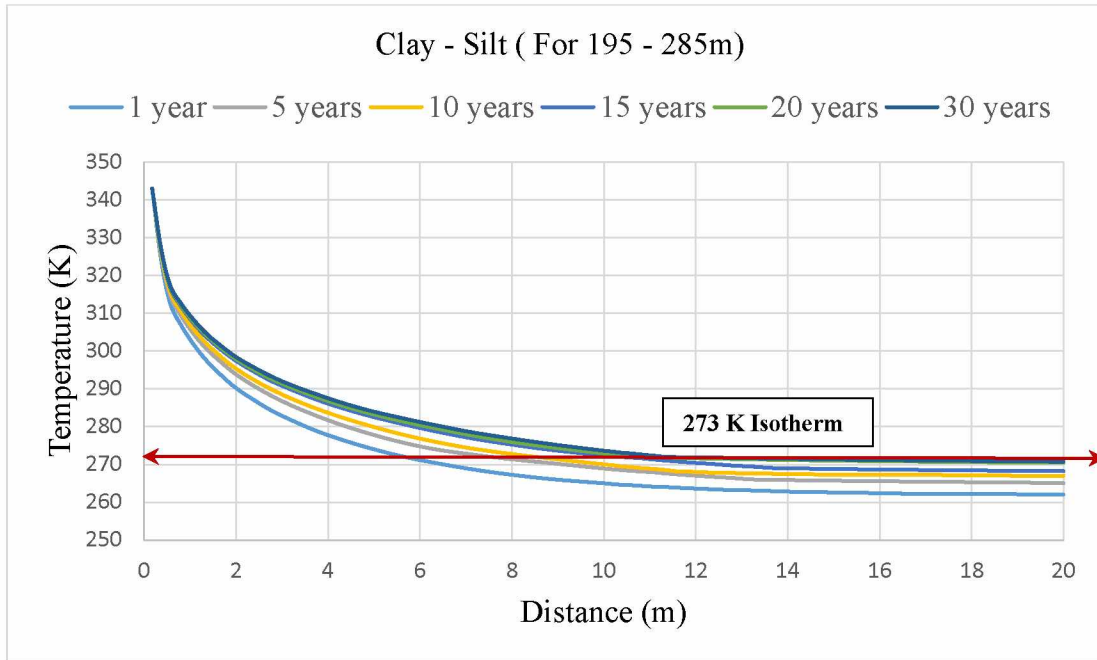


Figure 14. Clay - Silt : Temperature Distribution over a distance of 20 m from thr center of the wellbore

<i>Time (yrs.)</i>	<i>Thaw Radius (m) from small model analysis</i>
1	5
2	5.5
3	6.2
4	6.6
5	6.95
7	7.5
10	8
12	8.4
15	9
17	9.5
20	10
22	10.2
25	10.4
27	10.5
30	10.6

Table 8. Thaw Radius – Silt from the small model after applying boundary conditions

The following graphs show the temperature profiles to study the thaw radius at different times for the small model. We can see that the thaw radius increases rapidly over the first few years and then gradually slows down. More accurate values can be studied with the help of the thaw radius tables provided above in Table 9.

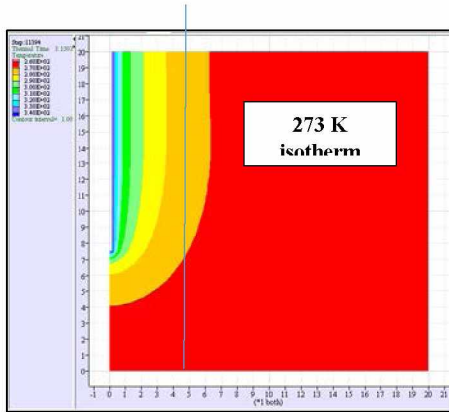


Figure 15a. 1 year Silt Profile

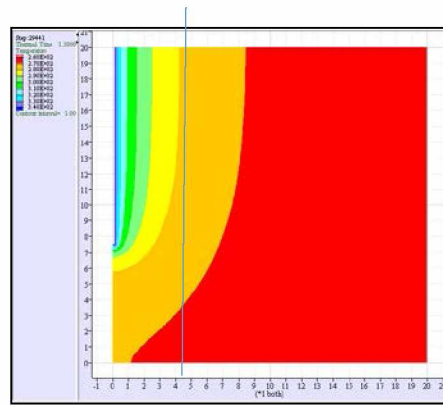


Figure 15b. 5 years Silt Profile

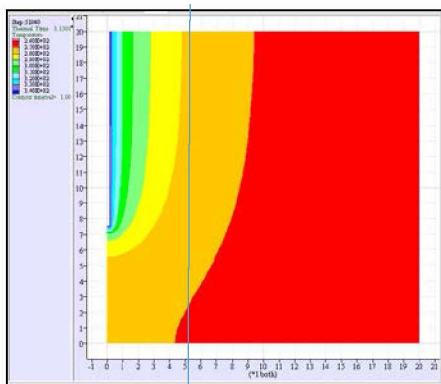


Figure 15c. 10 years Silt Profile

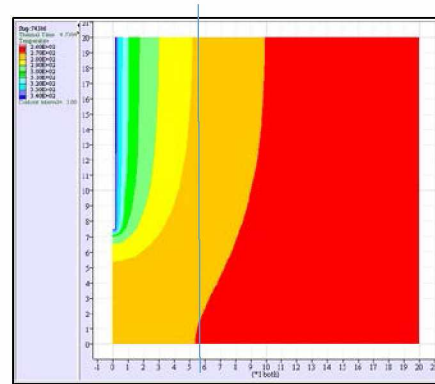


Figure 15d. 15 years Silt Profile

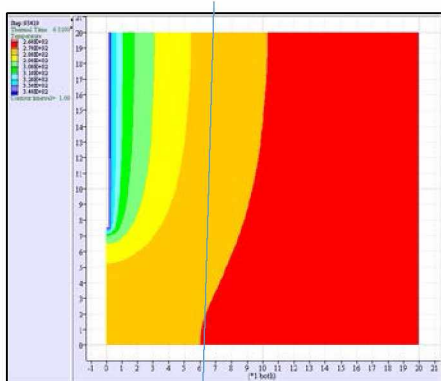


Figure 15e. 20 years Silt Profile

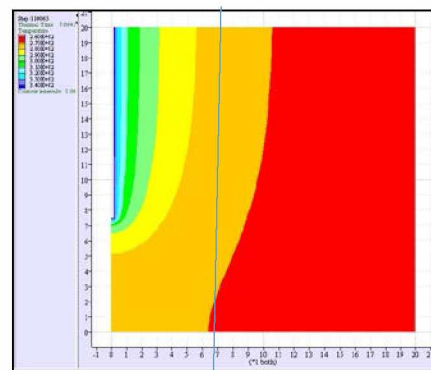


Figure 15f. 25 years Silt Profile

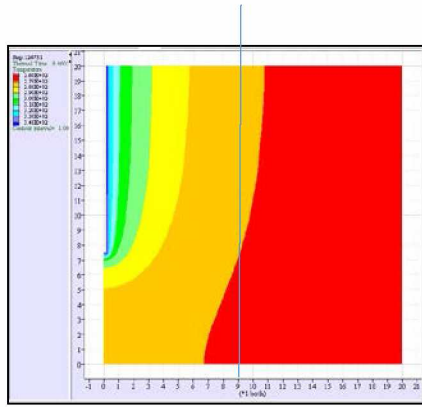


Figure 15g. 30 years Silt Profile

#### 4.4 Small Model Analysis: Model 3

The third model consisted of a cross-section of silt and sand at a depth of 280m to 300m. The temperature distribution for this model is shown in Figure 16. The main objective of this model was to simulate the temperature distribution 20 m from the center of the wellbore in a silt and sand cross-section taken from the big model. Further, also to develop correlations relating the wellbore temperatures and distance from the center of the wellbore.

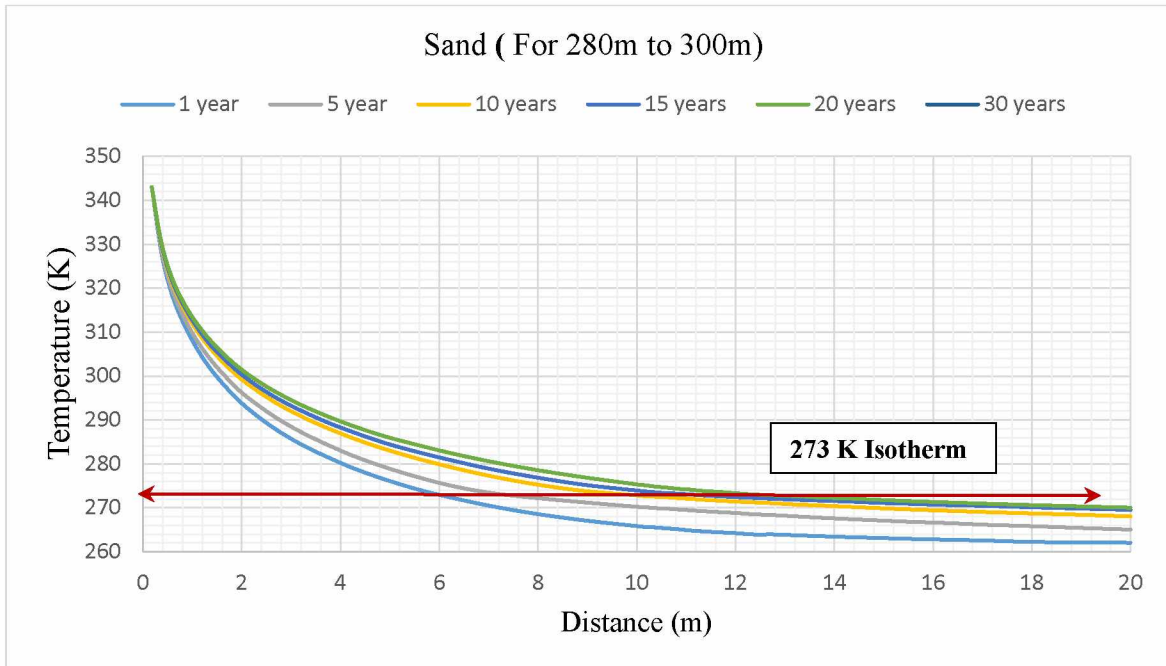


Figure 12. Silt-Sand Temperature Distribution over a distance of 20 m from the center of the wellbore



<i>Time (yrs.)</i>	<i>Thaw Radius (m) from small model analysis</i>
1	6
2	6.3
3	6.6
4	6.9
5	7.2
7	7.9
10	8.9
12	9.4
15	9.95
17	10.4
20	11.08
22	11.5
25	12
27	12.2
30	12.5

Table 10. Thaw Radius Silt – Sand from the small model after applying boundary conditions

The following Figure 17 shows the temperature profiles to study the thaw radius at different times for the small model of silt and sand. We can see that the thaw radius increases rapidly over the first few years and then gradually slows down. More accurate values can be studied with the help of the thaw radius table provided above (see Table 10).

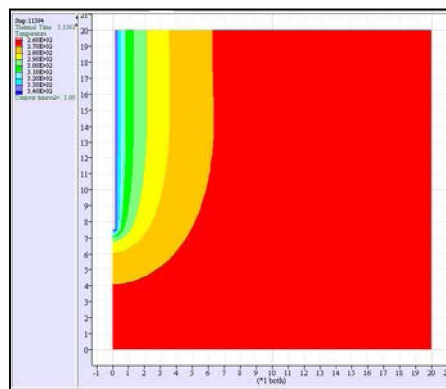


Figure 13a. 1 year Silt - Sand Profile

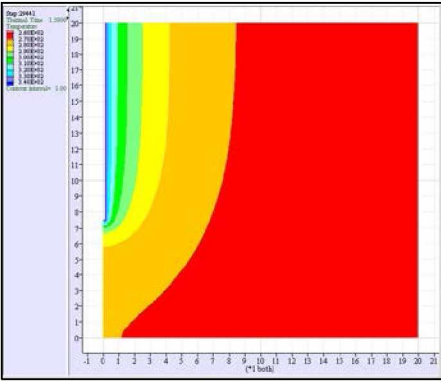


Figure 17b. 5 year Silt - Sand Profile

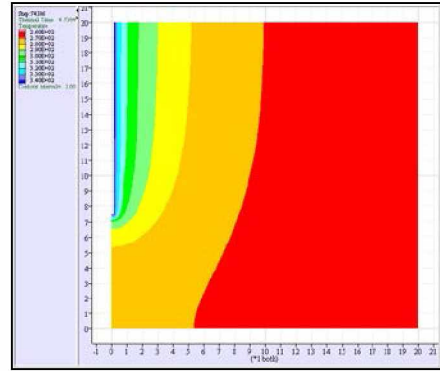


Figure 17c. 10 years Silt - Sand Profile

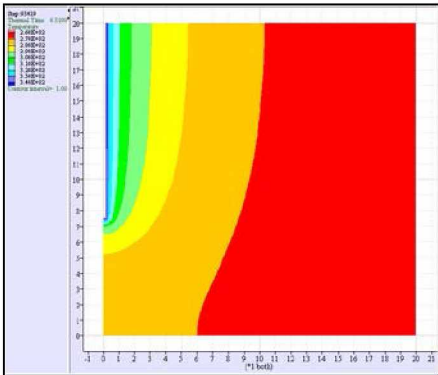


Figure 17d. 15 years Silt - Sand Profile

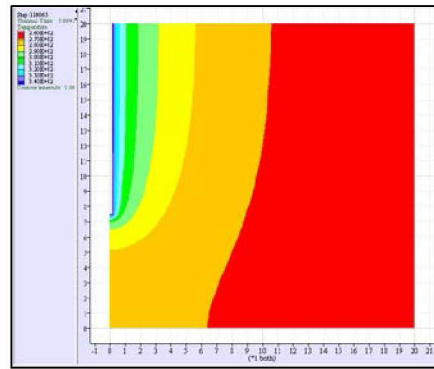


Figure 17e. 20 years Silt - Sand Profile

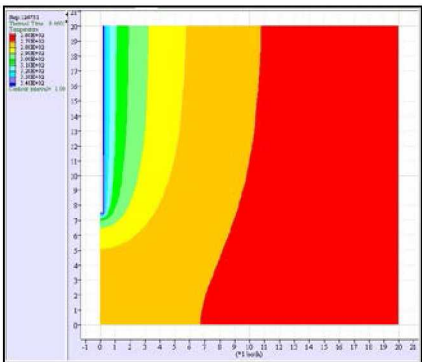


Figure 17f. 25 years Silt - Sand Profile

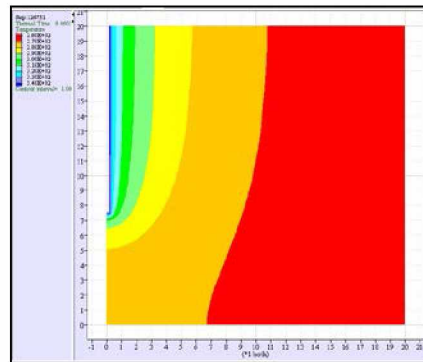


Figure 17g. 30 years silt - Sand Profile

A comparison of these soil sections was carried out to study the differences in thaw radius as shown in Figure 18. The Figure 18 below shows the thaw radius of a clay-silt cross-section and a silt-sand cross-section for 1 to 30 years only. Poly. (Sand) and Poly. (Silt) are the polynomial equations developed for each type of soil by Microsoft Excel to get a good curve fit with a high regression coefficient ( $R^2$ ) value of 0.99. Further, it can be observed that the thaw radius of the sand cross-section is higher than that of the silt. This is due to differences in thermal properties such as specific heat, thermal conductivity, and the latent heat.

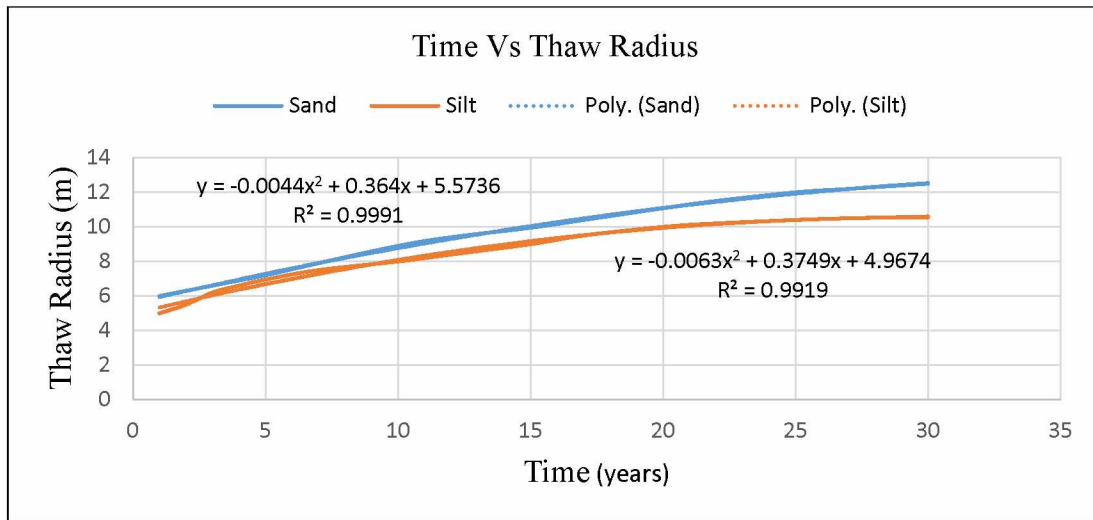


Figure 18. Time vs. Thaw Radius

Since clay has properties very close to that of silt, it was difficult to accurately determine the thaw radius of clay separately. The main reason for eliminating clay was because FLAC designates thermal values based on zones and since the values of silt and clay were close, it became hard to determine the exact values of the thaw radii. So, FLAC assigned the same values to the end points of each grid cell.

#### 4.5 Steam Injection

The three models were also tested to study the effect of steam injection on the formation over a period of 10 years. The temperature used for the investigation of steam injection was 383K. The results obtained were as follows.

#### 4.6 Big Model Results

Similar to 343K temperature analysis carries out initially the thaw radius and the temperatures at 20m determined from the big model are shown in Table 11. These thaw radii were obtained from the big model along with the boundary conditions for the small model as given in the table below.

<i>Years</i>	<i>Thaw radius (m)</i>	<i>Temp at 20m for the Boundary Conditions of the small model</i>
1	8	262
2	10.2	262.7
3	12.6	265.7
4	13.5	267.4
5	13.9	268.2
6	14.2	268.9
7	14.5	269.4
8	15	269.8
9	15.5	270.2
10	16	270.4

Table 9. Thaw Radius and boundary conditions for small model from Big Model (Steam Injection)

#### 4.7 Small Model Analysis

Figures 21 and 22 were obtained for sand and silt temperature distributions at 383 K. These figures were plotted mainly to get the near wellbore region upon injection of steam over the time span of 1 to 10 years. The 273 K isotherm line shows the increasing thaw radius over time of 10

years. The boundary conditions were used from the Big Model built for the steam injection analysis.

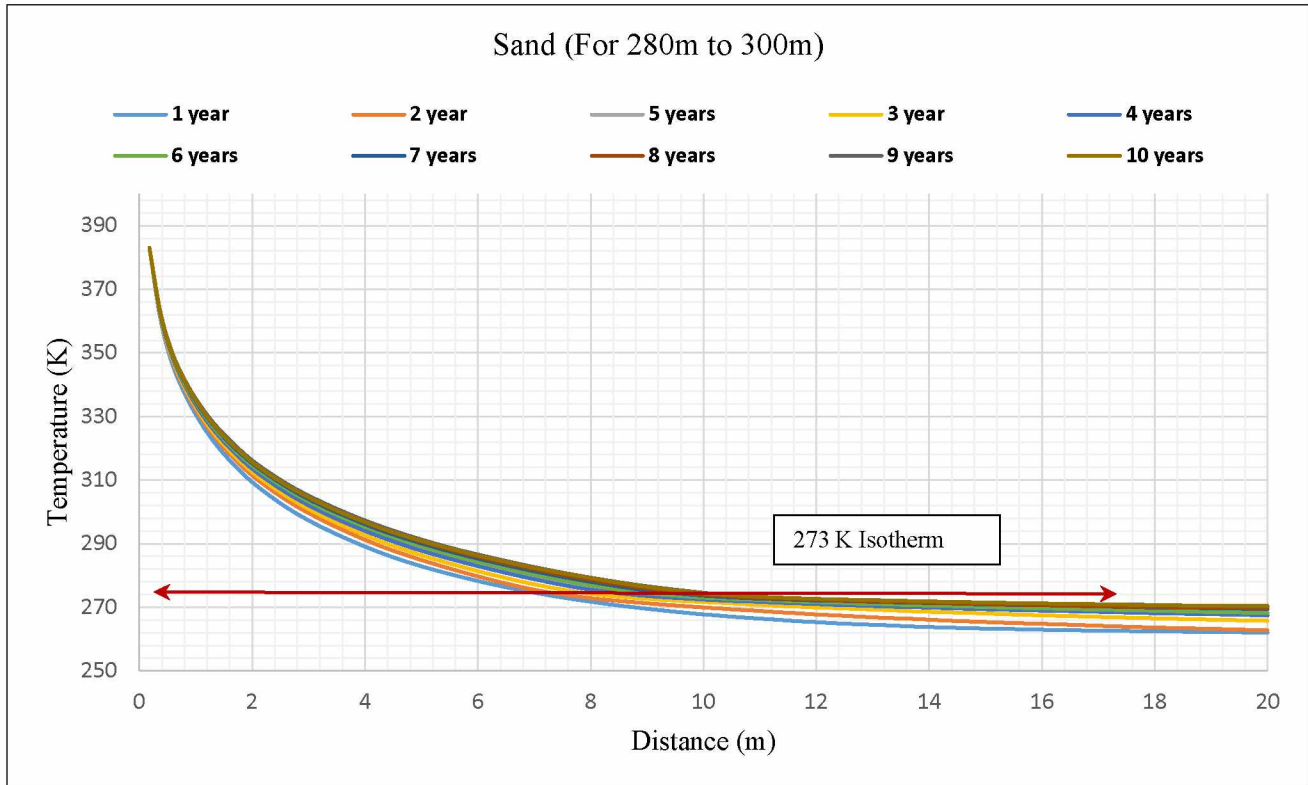


Figure 14. Silt – Sand : Temperature Distribution over a distance of 20 m from thr center of the wellbore Temperature Distribution Sand

Furthermore, a comparison was carried out between the thaw radius of silt and sand at wellbore temperatures of 343K and 383K. It was observed that the two curves followed the same trend but the curve with the wellbore temperature of 383K shifted towards a higher thaw radius. Equations were also obtained with the regression  $R^2$  values being above 0.99. The equations are shown in Figures 23 and 24.

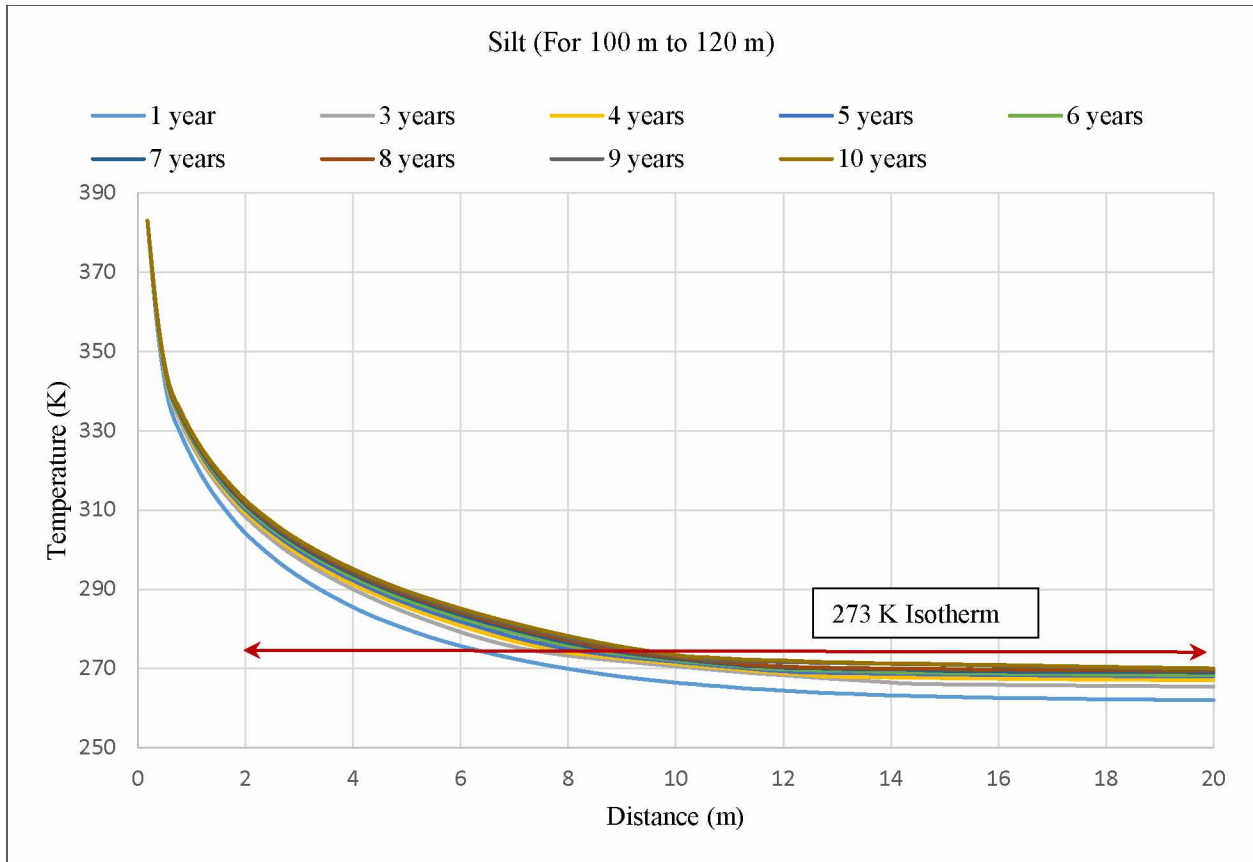


Figure 15. Clay - Silt: Temperature Distribution over a distance of 20 m from thr center of the wellbore Temperature Distribution Sand

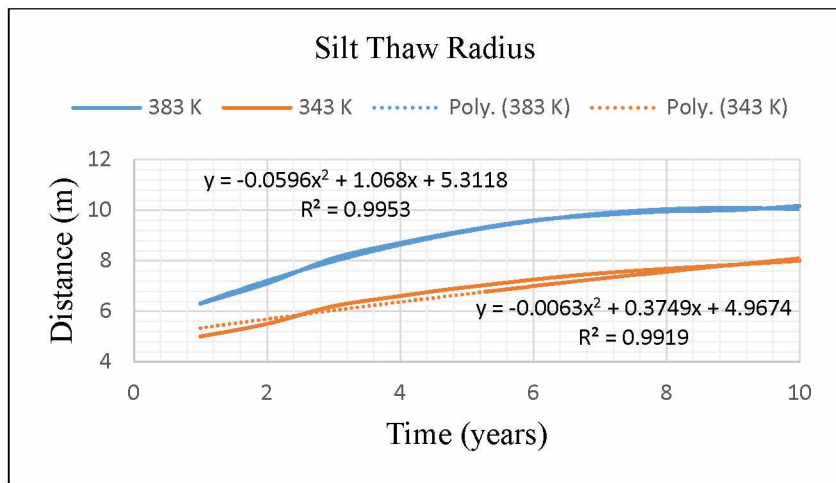


Figure 16. Silt Thaw Radius at 343 K and 383 K for comparison

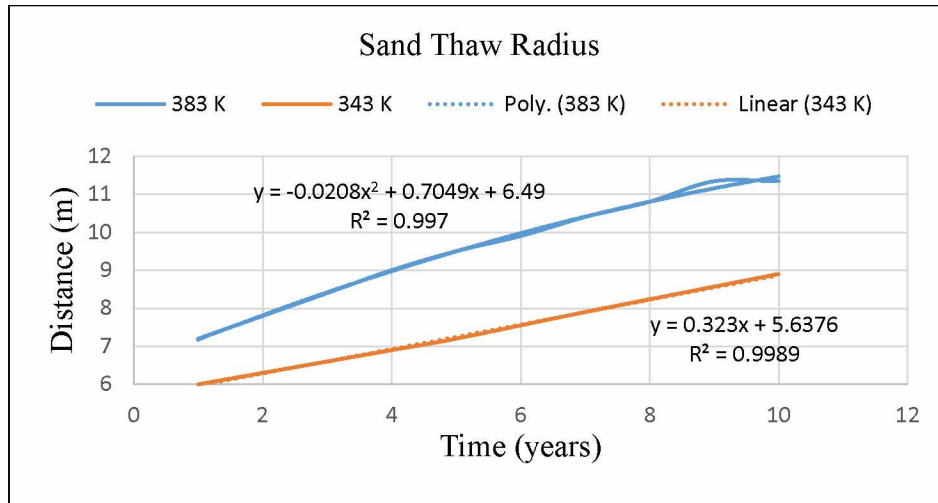


Figure 17. Sand Thaw Radius at 343 K and 383 K for comparison

#### 4.8 Sensitivity Analysis

In order to understand the reason behind the difference in the thaw radius of sand and silt, a sensitivity analysis was carried out. The three main thermal properties used as an input in FLAC were thermal conductivity, specific heat, and the thermal expansion coefficient. It was understood that changes in the thermal expansion coefficient and specific heat did not have a big impact on the thaw radius of the respective soils. Thus, the thermal conductivity was taken into account and the thaw radius for higher and lower values of thermal conductivity was simulated using the base model. This was done for both silt and sand. Figure 18 shows the thaw radius profiles for the base case at 343 K.

The conductivities used for sensitivity analysis are given in Table 12. The lower and higher values were taken into consideration randomly after studying the various ranges for each of these values (Johnston, 1981; Perkins 1979; Kresten, 1969). The alteration of the thermal conductivity of sand gave the thaw radius results as given in Table 13 and plotted in figure 26. Similarly, the thaw radius values for silt are given in Table 14 and plotted in figure 27.

<i>Soil Type</i>	<i>Conductivity (W/m K)</i>					
	<i>Base Case</i>		<i>Lower</i>		<i>Higher</i>	
	<i>Frozen</i>	<i>Unfrozen</i>	<i>Frozen</i>	<i>Unfrozen</i>	<i>Frozen</i>	<i>Unfrozen</i>
<i>Silt</i>	1.956	1.471	1.756	1.375	2.100	1.640
<i>Sand</i>	2.208	1.568	1.886	1.425	2.467	1.739

Table 10. Lower and Higher Conductivity Values for Sensitivity Analysis

<i>Time</i>	<i>Thaw Radius from sensitivity analysis</i>	<i>Thaw Radius from sensitivity analysis</i>	<i>Thaw Radius from sensitivity analysis</i>
<i>Years</i>	<i>Base Case Conductivity values</i>	<i>Lower thermal conductivity values</i>	<i>Higher thermal conductivity values</i>
1	6	5.8	6.3
2	6.3	6.1	6.7
3	6.6	6.35	7
4	6.9	6.7	7.4
5	7.2	6.9	7.7
7	7.9	7.6	8.2
10	8.9	8.6	9
12	9.4	8.9	9.6
15	9.95	9.57	10.1
17	10.4	10.1	10.6
20	11.08	10.6	11.3
22	11.5	10.95	11.7
25	12	11.4	12.1
27	12.2	11.7	12.3
30	12.5	11.9	12.6

Table 11. Sand: Thaw Radius from Sensitivity Analysis in response to changes in thermal conductivity



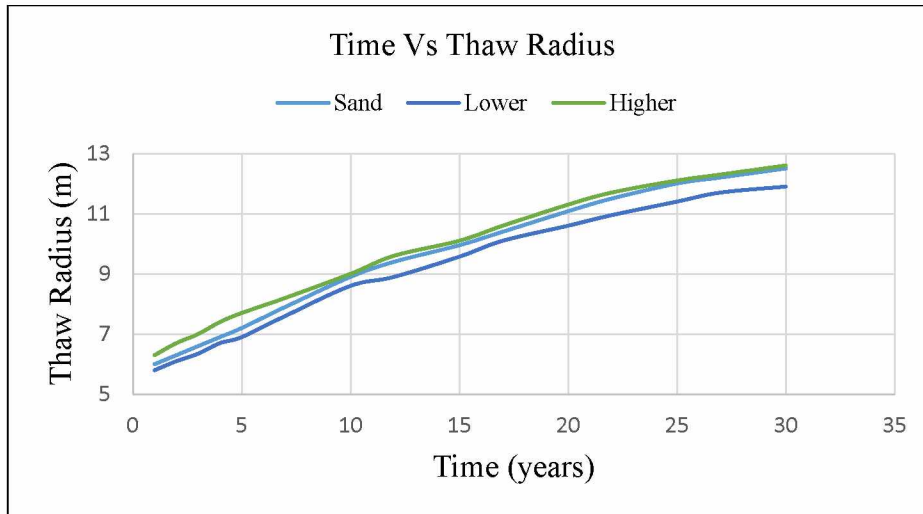


Figure 18. Plot of thaw radius for Sand sensitivity analysis of lower and higher values thermal conductivity values than the base case.

<i>Time</i>	<i>Thaw Radius from sensitivity analysis</i>	<i>Thaw Radius from sensitivity analysis</i>	<i>Thaw Radius from sensitivity analysis</i>
<i>Years</i>	<i>Base Case Conductivity values</i>	<i>Lower thermal conductivity values</i>	<i>Higher thermal conductivity values</i>
1	5	4.8	5.25
2	5.5	5.3	5.7
3	6.2	6	6.4
4	6.6	6.3	6.8
5	6.95	6.7	7.2
7	7.5	7.2	7.7
10	8	7.8	8.2
12	8.4	8.2	8.7
15	9	8.7	9.2
17	9.5	9.2	9.7
20	10	9.7	10.2
22	10.2	9.8	10.4
25	10.4	9.9	10.6
27	10.5	10	10.8
30	10.6	10.2	10.9

Table 12. Sand: Thaw Radius from Sensitivity Analysis in response to changes in thermal conductivity

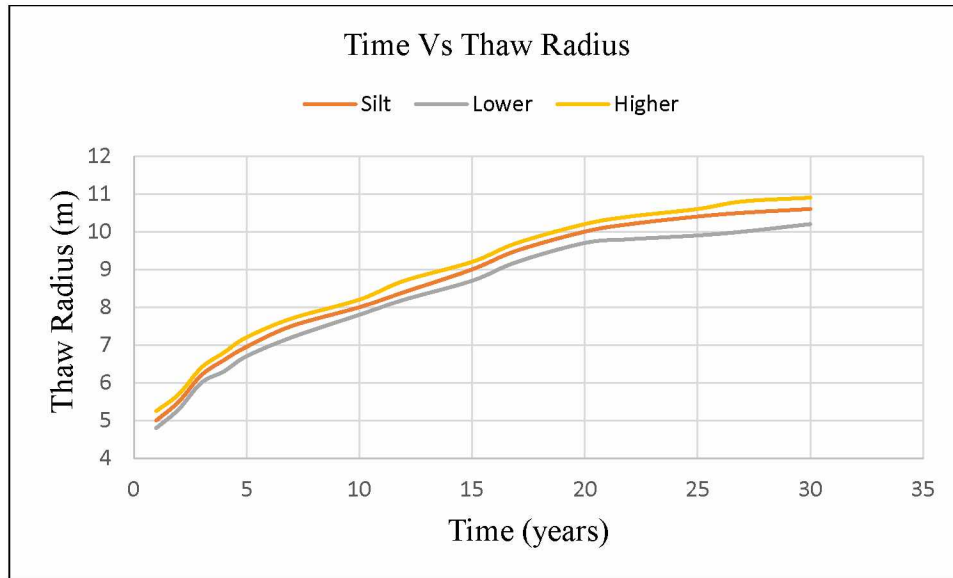


Figure 19. Plot of thaw radius for Silt sensitivity analysis of lower and higher values thermal conductivity values than the base case.

As we can see from the tables and graphs above of thaw radius for both silt and sand, the thermal conductivity plays an important role in estimating the thaw radius.

#### 4.9 Comparisons

A two-dimensional axi-symmetric geometry computer model was made in COMSOL Multiphysics™ software by Saurabh Suryawanshi (Graduate Student, University of Alaska, Fairbanks), using the heat transfer module. The model focused mainly on the heat exchange between the wellbore and surrounding frozen soils (permafrost) with time. It involved using temperature-dependent equation based inputs for the thermal properties of different frozen soils. Simulations were done for a period of 30 years for the analysis of thaw radius with time. The model built by Smith and Clegg (1971) is also an axi-symmetric model. However, other data and properties used by Smith and Clegg (1971) have not been given in the paper.

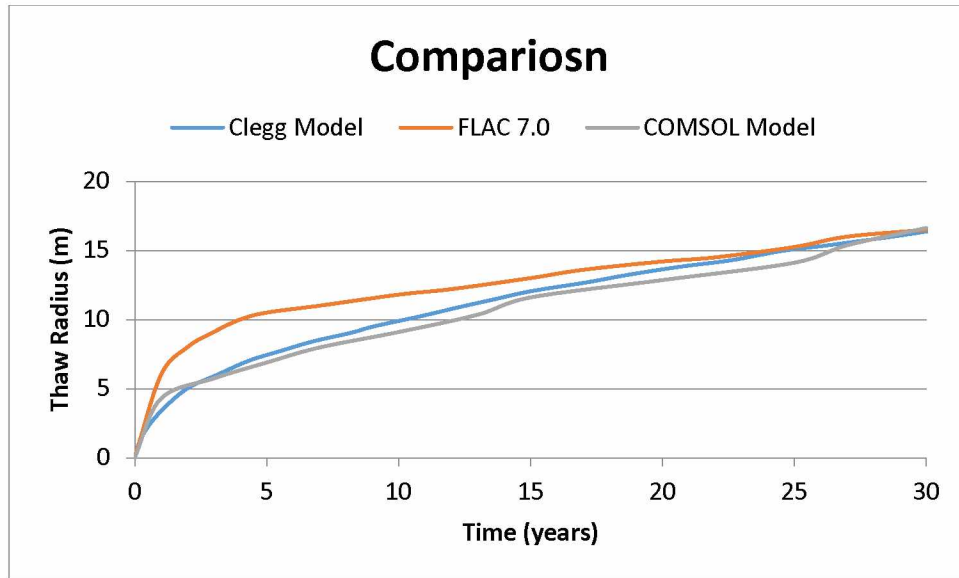


Figure 20. Comparison among different Models

The three models were compared (Figure 26). One of the reasons for the difference in the initial years was the difference in the input properties used in the three models. Also, when we notice the values of small models thaw radii of FLAC model and compare them with the thaw radii of Smith and Clegg (1971) and COMSOL models we observe that the thaw radii match well in the initial years, but do not match in the later years. Similarly, when the thaw radii of the big model of FLAC with Smith and Clegg (1971) and COMSOL models were compared we observed that the thaw radii do not match in the initial years but match in the later years. This may be due to the lateral extent of the big model being bigger than the small model resulting in more realistic boundary conditions. Hence, the model was large enough to predict more accurate transfer of heat through the permafrost. In the short term the big model most likely deviated as a result of the large mesh size with each grid cell being of approximately 1 meter in the near wellbore region. On the other hand, since the small model was an element of the big model, temperatures were obtained at a distance of 20 m from the wellbore in the big model and were imposed as boundary conditions in the small model. The small mesh size in the small model most likely

resulted into improved results in initial years. However, due to imposed boundary conditions, the results due not agree will with the other models in the later years. Hence, with the small model we get better results near the wellbore region, but as we move towards the boundary conditions over the span of 30 years the results become poor.

#### 4.10 Mitigation Techniques:

Engineers may approach design of permafrost completions in one of the two ways. The first strategy emphasizes well protection; the permafrost may be allowed to thaw but the design of wellbore completion should protect the wellbore from excessive stress. Second, and perhaps more conventional, the engineer primarily focusses on the protection of the permafrost via insulation (Merriam, 1975; Azzola et al.,2004).

In this project we tried to incorporate the second technique which was focusing on the permafrost via insulation. Since, the thaw radius of the near wellbore region was obtained from the Big Model in order to predict more accurate temperature distributions from the small models. Since, the grid cells of the Big Model were too big in width (1 meter) to incorporate a small insulation thickness (1.2 inch) of rigid polyurethane, aerogel or izoflex. Hence, in order to avoid wrong results insulation was not modeled.

## 5 CONCLUSIONS AND RECOMMENDATIONS

### 5.1 Conclusion

- 1) Estimating temperature distribution around the wellbore by using a thermal model to simulate thaw over a period of time will help maintain wellbore stability and integrity.
- 2) The current model built in FLAC can be used to simulate temperature distributions from the casing onwards with or without insulation and temperature distributions around the wellbore can be estimated using the correlations developed.
- 3) The main reason for the deviation in the FLAC model when compared to COMSOL model and Smith and Clegg (1971) could be the different input parameters considered in the three models. The COMSOL model used correlations for thermal conductivities and specific heat capacities. These correlations required water content values; those we used were obtained from the experiments carried out by the Department of Petroleum Engineering at the University of Alaska, Fairbanks.
- 4) The difference in thaw radii of FLAC model when compared with the thaw radii of Smith and Clegg (1971) and COMSOL model may be due to the lateral extent of the big model being bigger than the small model. Hence, the model was large enough to predict more accurate transfer of heat through the permafrost. In the short term the big model most likely yielded to large results due to the big mesh size. On the other hand, the small mesh size in the small model most likely resulted into matching of results in initial years but due imposed boundary conditions the results are low as compared to the other models in the later years. Hence, with the small model we get better results near the wellbore region but as we move towards the boundary conditions over the span of 30 years the results become low.

- 5) Different curves for steam injection were also simulated for sand and silt and thaw radius along with temperature distributions were obtained. The correlations can be used for estimating the near wellbore temperatures for a time span up to 10 years.
- 6) Insulation analysis (rigid poly-urethane, izoflex and aerogel) and different types of cement were attempted, but due to the limitation of grid thickness in the big model, they could not be carried out further. The big model was used to simulate temperatures for small models. Hence, taking temperatures from the big model without insulation and using them in small models with insulation could lead to a great amount of inaccuracy. In order to avoid these inaccuracies, this simulation was not carried out.

## 5.2 Recommendations

- 1) Insulation around the tubing or the wellbore can be studied. The current model could not model it because of the dimensions of the grid cells in the big model. Taking temperatures from the big model and applying them to the small model was not possible in the case of insulation. To avoid inaccuracy, these simulations were tried but not included in the report.
- 2) Thermal analysis that includes estimating the collapse pressure resulting from thawing can also be incorporated. It was not done in this model because the casing is defined in the non-failure mode. Hence, the casing will never fail/collapse irrespective of the stresses acting on it.
- 3) A single 3-dimensional model can be attempted in a different software package that includes stresses, strains, and thermal analysis to give more accurate results. This will help in estimating more relevant results with respect to the amount of stresses and the resulting thaw bulbs around the wellbore over a period of time.

- 4) Further, to make the model more realistic a case study can be taken into consideration which has accessible data and the temperature distribution can be matched with real time data from the field.

## 6 REFERENCES

1. Azzola, J. H., Pattillo, P. D., Richey, J. F., & Segreto, S. J. 2004. The Heat Transfer Characteristics of Vacuum Insulated Tubing. Society of Petroleum Engineers, Houston: pp 169-184
2. Bunton, M. A. 1999. Vacuum Jacketed Tubing: Past, Present, and Future. Society of Petroleum Engineers, doi:10.2118/55994-MS. Anchorage, Alaska: pp 306-313
3. Davies, B. E., 1979. Deep Permafrost Oil Production: The First two years. WPC Conference Paper 18201, Dundee, Scotland: 235-239
4. EIA.gov, "Annual Energy Outlook 2012", [http://www. Eia.gov/foecasts/aeo/er/index.cfm](http://www.Eia.gov/foecasts/aeo/er/index.cfm), (accessed Sept.23, 2013)
5. G. H. Johnston and F. L., Permafrost Engineering and Design Construction, 1981. Wiley and Sons Toronto:540-586 p.
6. Hirshberg, A. J., Moyer, M. C., & Rickenbach, R. M.1988. Surface-Casing Strain Capacity for North Slope Operations. Society of Petroleum Engineers, Houston: pp 289-292
7. Howell, E. P., Seth, M. S., & Perkins, T. K. 1972. Temperature Calculations for Wells Which Are Completed Through Permafrost. Society of Petroleum Engineers, San Antonio: pp 211-217
8. Jeuren Xie, 2009. Analysis of Thaw Subsidence Impacts on Production Wells, CFER-Technologies, SPE Arctic and Extreme Environments Conference & Exhibition, Edmonton, Alberta, Canada: pp 3-5

9. Kresten, 1969, Engineering Characteristics of Frozen and Thawing Soils - Properties of frozen and thawing soils. Russia: pp 308-311
10. Lin, C. J., & Wheeler, J. D. 1978. Simulation of Permafrost Thaw Behavior at Prudhoe Bay. Society of Petroleum Engineers: pp 461-465
11. Matthews, C. M., & Zhang, G. 2012. Importance of Deep Permafrost Soil Characterization for Accurate Assessment of Thaw Subsidence Impacts on the Design and Integrity of Arctic Wells. Offshore Technology Conference, Houston: 3 p
12. Mitchell, R. F., & Goodman, M. A. 1978. Permafrost Thaw-Subsidence Casing Design. Society of Petroleum Engineers: pp 17-45
13. Malcolm A. Goodman, 1977. How permafrost thaw/freeze creates wellbore loading. Energetech Engineering and Research Co., Houston: pp 641-645
14. Marques, C., Castanier, L. M., & Kovsky, A. R. 2009. Thaw Front Dynamics and Super Insulated Well for Thermal Recovery in Cold Environments. Society of Petroleum Engineers: pp 411-417
15. Merriam, R., Wechsler, A., Boorman, R., and Davies, B. 1975. Insulated Hot Oil-Producing Wells In Permafrost. Society of Petroleum Engineers, Alaska: 5 p
16. Smith, R.E., and Clegg, M.W. 1971. Analysis and design of production wells through thick permafrost. Proceeding 8<sup>th</sup> World Petroleum Congress, Moscow: pp. 380-387.
17. N. A. Tsytoich, 2000. The mechanics of frozen ground. Volume 2: 33 p
18. Paolo Gardoni, 2011. Structural Reliability : Assessing the condition and Reliability of Casing in Compacting Reservoirs. Texas A&M University: 543 p



19. Skoczylas, P. and C-FER Technologies. 2012. A Review of Methods for Calculating Heat Transfer from a wellbore to the surrounding Ground. Paper WHOC12-240 presented at the World Heavy Oil Congress, Aberdeen, Scotland: pp 6-11
20. Singh, Probjot et al. 2007. An application of Vacuum-Insulated Tubing (VIT) for Wax Control in an Arctic Environment. SPE Journal Paper 111006: pp 3-6
21. Vassilellis, G. D., Capper, L., Schneider, M. J., & Kuhlman, M. 2013. Downhole Burners: Pushing the Envelope of Enhanced Oil Recovery in the Arctic. International Society of Offshore and Polar Engineers. June: 5 p
22. Wilson, W. N., Perkins, T. K., & Striegler, J. H. 1979. Axial Buckling Stability of Cemented Pipe. Society of Petroleum Engineers. doi:10.2118/8254-MS. January: 7 p
23. Xie, J., & Matthews, C. M. 2011. Methodology to Assess Thaw Subsidence Impacts on the Design and Integrity of Oil and Gas Wells in Arctic Regions. Society of Petroleum Engineers. October: pp 18-24